DUKE ENERGY
FLORIDA

Matthew R. Bernier
ASSOCIATE GENERAL COUNSEL
Duke Energy Florida, LLC

May 23, 2019

VIA ELECTRONIC FILING

Adam J. Teitzman, Commission Clerk
Florida Public Service Commission
2540 Shumard Oak Boulevard
Tallahassee, Florida 32399-0850

Re: *Duke Energy Florida, LLC's Demand Side Management Annual Report for Calendar Year 2018*; Undocketed

Dear Mr. Teitzman:

Please find enclosed for electronic filing Duke Energy Florida, LLC's Response to Staff's First Data Request (Nos. 1-6).

Thank you for your assistance in this matter. Please feel free to call me at (850) 521-1428 should you have any questions concerning this filing.

Sincerely,

/s/ Matthew R. Bernier

Matthew R. Bernier

MRB/cmk
Enclosures

cc: Tripp Coston
Charles Morgan II

106 East College Avenue, Suite 800 ▪ Tallahassee, Florida 32301
Phone: 850.521.1428 ▪ Fax: 727.820.5041 ▪ Email: matthew.bernier@duke-energy.com

Duke Energy Florida, LLC's Response to
Staff's First Data Request regarding Duke Energy Florida, LLC's
2018 Demand-Side Management Annual Report

1. Please describe the Company's process for monitoring any new federal energy efficiency standards and Florida Building Code requirements, including how the Company modifies existing programs to reflect these changes, if necessary (21^{st} and 22^{nd} Semi-Annual Reports to Congress on Appliance Energy Efficiency Rulemakings issued in 2018).

Response
DEF's approach for monitoring any new federal energy efficiency standards and Florida Building Code requirements involves both internal and external resources. DEF stays informed about new federal energy efficiency standards and Florida Building Code requirements through participation in trade associations, industry groups, and building associations. DEF also stays informed about new technologies through meetings with peer utilities and review of regulatory filings.

DEF's internal Technology Evaluation team also researches and evaluates new DSM technologies as they become available in the marketplace to identify potential program opportunities. This is a rigorous process that involves further analysis of both customer and company costs and benefits, projected participation levels, analysis of cost effectiveness test results, discussion of operational considerations, and customer rate.

DEF modifies existing programs to reflect these changes, if necessary; Recently, The Commission approved two proposed modifications to DEF's Better Business Program. The first was for air cooled and water-cooled chillers. The need for the modifications was driven by updates to the minimum efficiency requirements in the Florida Building Code that went into effect January 1, 2018. The second approved modification was to the processes for incentive payments to customers. This change allows DEF to pay incentives directly to Trade Allies provided the customer provides signed authorization conveying the incentive to the Trade Ally or if the Trade Ally discounts the incentive on the invoice at the point of sale. Incorporating this change streamlines the process for providing incentives to customers.

2. Please provide a detailed description of the Company's research and development initiatives, including the status of each project and any final reports related to the work completed under this DSM program.

Response
Technology Development Initiatives - January 2018 - December 2018:
Several research and development projects continued and/or launched in 2018.

- Continued a project for appliance energy efficiency and demand response using the CTA-2045 modular communications interface including field pilot projects for CTA-

2045-enabled retrofit water heater switches, resistance and heat-pump water heaters, pool pumps, HVAC thermostats and electric vehicle chargers (EVSE). The purpose of the project is to understand the potential to utilize the CTA-2045 device to support load management programs. DEF plans to continue to collect and analyze field pilot data for design of potential cost-effective demand response programs.

- Completed a project with the University of South Florida for commercial building energy efficiency and demand response utilizing control systems that interface with existing customer building management systems. A final report for this project was produced in 2018. Duke is investigating the cost-effectiveness of a potential Custom Program for this technology. Please see Attachment A for final report.
- Completed a demonstration of technologies that utilize Variable-Speed Heat Pumps with the potential of eliminating strip heat as a back-up heat source for heat pumps. Significant improvements in energy efficiency have been documented at these sites. A final report was produced in 2018. Preliminary cost-effectiveness proved to be marginal due to the high initial cost of the Variable Capacity Heat Pump systems. Please see Attachment B for final report.
- Completed the Renewable SEEDS project. This project consisted of two sites with PV systems integrated with energy storage. Both sites have demonstrated smoothing, energy shifting and demand response capabilities. A final report summarizing the results was completed. Please see Attachment C for final report.
- Continued a project with the University of South Florida to leverage customer-sited solar PV and energy storage at the USF 5th Avenue Garage Microgrid. The system provides load smoothing, islanding and demand response. A publicly available dashboard that shows live data, project specific facts and the capability of downloading data for further study is available for the site at https://dashboards.epri.com/duke-usfsp-parking. Results of this research will be used for design of a potential cost-effective demand response program.
- Continued the EPRI Solar DPV project for data collection to document customer solar resources with a focus on larger PV arrays with and without energy storage. This project also provides the data stream for the dashboard mentioned above.
- Continued participation in an EPRI project to study the potential of using customer demand response to compensate for variable loads and intermittent renewable generation resources.
- Continued the Energy Management Circuit Breaker Project. This project continued to explore the potential for developing a program for customer circuit breakers that includes communication, metering, and remote operation for potential applications including energy efficiency, demand response, and integration of distributed energy resources. A field pilot program has been installed and operational data is being collected from appliances in 10 customer homes. This data will be used to document the operation of these breakers and assess the cost-effectiveness for potential EE and DR programs.
- Partnered with EPRI on a project to assess the demand response opportunities for new and existing variable capacity heat pump systems for potential future load management programs. We continued implementation of a pilot to use manufacturer cloud communications to control existing variable-capacity heat pumps. This pilot will

assess the viability of communications and impacts of variable capacity heat pumps for demand response and energy efficiency.

- Launched a project to gather robust data about residential customers that drive electric vehicles. The project will determine what type of hardware the customer uses to charge their vehicle, where they do their charging (at home, work or public charging station, in/out of DEF service territory, etc.) and how much power and energy are consumed by EV charging. The project will also assess the capability of EVs to be a demand response resource.
- Launched a project that will provide knowledge in methods to utilize customer Wi-Fi infrastructure to develop a dedicated, durable and secure utility communication channel to connected devices. The project will also provide knowledge on the effectiveness of Wi-Fi signal strength improvement technology. This technology could lead to lower costs and improved cost-effectiveness for existing and future demand response and energy efficiency programs.
- Partnered with EPRI and other research organizations to evaluate energy efficiency, energy storage, and alternative energy / innovative technologies.

3. Please describe any changes the Company has made to its process for ensuring low-income customers are aware of, and have access to, conservation programs.

Response
DEF informs low income customers about low cost and no cost energy efficiency measures and incentives that they may be eligible for in a number of ways, including through residential audits, community meetings, home shows, bill stuffers, emails, direct mail, home energy reports, and through its website.

In 2017, the Company changed the guidelines for the Low Income Weatherization Program to include more low income customers by better aligning with the agencies' definition of low income (200% of poverty, 60% of area median income, etc.). In 2018, the program manager met with a large group of agencies performing work for low income housing to ensure that they were aware of the program offerings for low income customers.

In 2018, DEF also modified its low income programs to begin providing LED lightbulbs instead of CFL's and increased the number of bulbs from 5 to 8.

4. According to Page 10 of the report, DEF approved 29 projects in the Florida Custom Incentive program in 2018. Please provide the details for each project's scope, including the measure(s), its overall project costs, the cost-effectiveness test results, and the amount of incentive paid.

Response
Please see Attachment D.

5. The following programs fell below the Company's initial projected participation penetration levels:

   a. Please describe the Company's assessment on why it did not achieve the projected participation levels for 2018.

   b. Is the Company considering or researching any program modifications to ensure these programs are able to more closely achieve the projected participation levels? Please explain.

   <u>Response</u>

   Low Income Weatherization

   a. The LIWAP program is operated through the local weatherization assistance agencies. Over the years, new personnel at these agencies have not shown the same level of interest in participating in the program as their predecessors. Despite attending weatherization conferences and meeting directly with agency staff, participation continues to wane.

   b. Yes. In 2017, the Company changed the guidelines to include more low income customers by better aligning with the agencies' definition of low income (200% of poverty, 60% of area median income, etc.). As a result of this change, we have been adding more agencies that are now eligible to receive the incentives. In 2018, the program manager met with a large group of agencies performing work for low income housing, as detailed below. Of these agencies, 6 have agreed to sign a Memo of Understanding to receive these incentives through this program.

      Lake County Community Development, St Pete Housing, Osceola County Housing, NF Regional Housing Authority, NF Community Weatherization Network, Habitat for Humanity, Pasco County Community Development, Homes N Partnership, Rebuild Orlando Together, Rebuild North Fl. Together, Apple Air & Heating, Levy County Housing, Lift Orlando, Ability Housing, Alachua County, Marion County, Hardee County Housing, Seminole County Community Development, Colonial Hills Association, Volusia County, Hernando County, Rebuild Tampa Bay, US Dept. of Housing Urban Development, Catholic Charities, Fl. SPECS, City of Wildwood, City of Deland, Neighborhood Housing & Development Corporation, the Goodwin Group

   Residential Energy Management

   a. The residential demand response program was implemented in 1981 and currently approximately 435,000 residential customers, representing 27% of DEF's total residential customers, already participate in the program. Despite significant marketing efforts over the past few years, DEF has not been able to achieve the level of participation anticipated in the last goals setting proceeding. DEF believes this is primarily due to market saturation issues.

b. Because DEF has not been able to meet the projected participation levels for the residential energy management program for the past few years, DEF adjusted its internal goals for the other residential programs to ensure that the overall residential goals were met.

Better Business

a. Although the reported participation for the Commercial programs was significantly less than the projected participation, the demand and energy savings from the Better Business program well exceeded the projected savings included in the Program Plan. There is a wide diversity in both the types of commercial customers and the demand and energy requirements of those customers. The types of measures incentivized through the Better Business program are often a bigger driver of program achievements and cost effectiveness than the actual number of participants.

b. DEF will continue to ensure that all customers are aware of opportunities through the Better Business program.

6. Please provide the number of participants for each type of energy audit completed during 2018:

<u>Response</u>

Residential
Free Walk-through – 16,284
Customer Online – 7,861
Customer Phone-Assisted – 10,755
Home Energy Rating – 0

Commercial/Industrial –
Walk-Through - 665
Phone-Assisted - 3

BuildingIQ Demand Response Program at University of South Florida Harbor Hall

I. Introduction

BuildingIQ (BIQ) hardware interfaces with a customer's building management system (BMS), receiving input from BMS sensors and provides output to control equipment operation. The software technology platform is a cloud-based system which pulls data in real time from the BMS and weather data sources. BIQ reduces energy use on a continual real time basis for year-round energy savings and can also provide demand reduction during Demand Response (DR) events. The energy savings and demand reductions are achieved through proprietary, model-based, continuous reset strategies that target the zone temperature, the supply air temperature, and the duct static pressure in the HVAC systems. Thermal comfort of the client spaces is determined by the building operators in conjunction with BIQ. Allowable ranges of temperatures are maintained in accordance with ASHRAE thermal comfort standards and are determined and adjusted on an on-going basis. BIQ collects data from the BMS which it uses to develop baselines for optimizing the HVAC systems beyond what the BMS can provide. This report presents results from multiple DR events conducted at USF Harbor Hall showcasing the potential of this technology to reduce electricity demand in Florida.

II. BuildingIQ Deployment Process

The following are the primary aspects of a BuildingIQ deployment process:

1. IT Connectivity

a. Establishing the BuildingIQ Appliance as hardware provided by BuildingIQ, or approved hardware or VM provided by the facility, and enabling communications to our Portal and VPN access for our Operations team. BuildingIQ's Appliance was installed and started collected data on March 1st 2015.

Note that connectivity was interrupted from December 4th 2015 to February 10th 2016 due to an extensive renovation process at USF Harbor Hall.

2. Metering

a. Historical Data: Whole building historical data in 15-minute interval kW or kWh. Sub 15-minute data is acceptable. 1 year or more data if possible.

b. Live Feed: If existing meter is data enabled, we will make efforts to integrate with that system. If that is not possible, we can introduce our own pulse counter or CT and trending solution to collect that data in real time and send back to our cloud.

Real-time whole building data was available for USF Harbor Hall. The power meter BACnet point was mapped into the BuildingIQ system and historical data was uploaded to BuildingIQ's cloud.

c. Utility Details: We need copies of a few utility bills that overlap with the historical, for validating meter feed and determining tariffs. Be certain to specify if generation and supply are billed separately.

Harbor Hall facility personnel did not have access to utility bills.

3. Building Information

a. Drawings: Mechanical as-builts, electrical distribution diagrams, floorplans.

b. Equipment list: If a detailed list is maintained, it is useful to help determine what equipment we want to monitor. Sequence of Operations or design specifications are helpful, especially for non-standard or retrofitted systems.

c. Points List: If possible, we would like an export from the BMS detailing controllers, points, and if a controller is BACnet enabled on its own.

4. Remote Access to BMS

a. Having familiarity and an understanding of the BMS is important. We request a “read only” user account to grant us access to the GUI or front end of the BMS. As these systems are typically only accessible via a local connection, we will use our VPN to connect to our Appliance and then login to the BMS. BMS access allows BuildingIQ operators to determine the root cause of performing issues, but it does not prevent the system from resetting setpoints.

Remote BMS access through a user interface was not available for this site.

5. BACnet Communications

The ability for our Appliance to have read/write communications with the BMS is critical, and our Appliance is strictly capable of BACnet/IP communications.

a. Communication with the equipment and BMS needs to happen over BACnet/IP. Not all devices specifically need to be BACnet/IP capable, but they must be in communication with an exporting device or front-end that is.

b. BuildingIQ will be reading several points from the BMS, our polling frequency is typically every 2-3 minutes but can be configured if necessary. Typical equipment monitored includes AHUs, VAVs and terminal units, and large plant equipment such as chillers, boilers, and condensers. A general points list will be provided to begin scoping the work. More specific points will be determined using the BMS and data gathered on our site visit.

c. BuildingIQ will be writing to two primary AHU setpoints, Supply Air Temperature SP and Supply Static Pressure SP. Our Appliance is configured to write at the same BACnet priority for each point (typically 11) and we release our setpoints by writing “null” at that same priority. This effectively scrubs our value and returns to previous value. If BACnet priority is not used, then control logic must exist to allow the BuildingIQ setpoints to be toggled on and off.

In the case of USF Harbor Hall, BMS programming changes were necessary to allow the BuildingIQ system to control the supply air temperature/pressure setpoints for the multizone units and the zone temperature setpoints for the single zone units. The BMS contractor (CSSI) created new points in the BMS where the BuildingIQ system could write to and programmed switches that allowed the building operator to release control back to the BMS if needed.

d. BuildingIQ will be writing setpoints to control VAVs and terminal units. The goal is to have total control over the setpoints that the VAVs are using during occupied hours. Depending on equipment, this may include cooling and/or heating setpoints or a deadband. Depending on individual heating or cooling mechanisms on individual terminal units, we may need a switch that can “lockout” this function.

III. BuildingIQ Summer and Winter DR Strategy

BuildingIQ Demand Response reset strategies are able to significantly reduce the power demand from cooling or heating systems for specific periods of time while maintaining certain comfort level. The DR sequence of operation is constituted by three stages: pre-cooling/pre-heating, dispatch, and post-dispatch. During pre-cooling (pre-heating), colder (warmer) air is sent to the space to ensure comfort levels and maximize demand reduction at the beginning of the event. Throughout dispatch, the DR strategy adjusts the supply air temperature and pressure setpoints to reduce the compressor/chiller plant cooling loads and minimize fan power when the event is schedule in summertime. Modifications to low level setpoints guarantee the fastest equipment response with an immediate demand reduction. In the case of winter DR, the heating setpoints are decreased to minimize electric reheats at the AHU/VAV level. Zone temperature maximum and minimum limits are defined to avoid uncomfortable conditions for the occupants. After the event concludes (post-dispatch), the setpoints are slowly ratchet up or down to pre-event conditions to avoid a significant increase in demand and return the spaces back to their regular comfort levels. Even though the system is completely automated and customizable, BuildingIQ personnel monitor the events to address potential comfort issues or increase demand reduction if feasible.

The demand drop potential of each building depends on different sites characteristics suchs as size, type of systems being controlled by BuilndingIQ, and the tenant's comfort tolerance. The DR capacity for each building is determined by performing three DR events; one at 10% of expected capacity, the second at 50% and the third at 100% of expected capacity. These test events allow BIQ to determine the total DR capacity of each facility. An average baseline is developed using the three days of the prior ten non-holiday weekdays (which were not event days) with the highest average hourly demand during the period of 3:00 PM to 7:00 PM. The average baseline is normalized to the event day by offsetting the baseline profile to match the event day profile for a period prior to pre-cooling/pre-heating. The normalizing occurs for a one-hour period, two hours prior to the start of the event. The demand reduction is then calculated as the difference between the baseline and the event day recorded demand during each event half an hour.

1. Harbor Hall

Harbor Hall is a 30,476 square foot building located in the University of South Florida campus in St. Petersburg. The site went through a major renovation process on 2015 and it has been fully operational with the new configuration since January 2016. The HVAC system is constituted by four single zone rooftop units (RTU-1, 6, 8, and 9) and five multi-zone rooftop units with two compressors and hot gas reheats (RTU-2, 3, 4, 5, and 7). Variable air volume boxes with electric reheats are coupled to the multi-zone rooftop units to provide conditioned air to office spaces, storage, meeting rooms, and classrooms. RTU's outside air dampers modulate to maintain standard air quality levels in the spaces. Occupancy in the offices spaces is constant while it varies in meeting rooms and classrooms depending on the class and event schedules.

Prepping Harbor Hall

In order to fully implement the summer/winter DR strategy at the building, different issues were addressed in terms of BMS programming and equipment response. Even though BuildingIQ started collecting data on April 6th 2015, the BuildingIQ system was controlling only three out of eight units during the summer of 2015 due to BMS programming issues. In fall 2015, the building entered a construction phase that resulted in a reconfiguration of the interior space and the HVAC system serving them. Due to the new configuration, a new implementation process was carried out to reestablish data flow and writing capabilities.

After the redeployment process was concluded, BuildingIQ was in control of the supply air temperature and pressure setpoints only at the multizone units (RTU-2, 3, 4, and 7) with data streaming issues at RTU-5. The BMS contractor (CSSI) had to introduce changes to the programming to allow BuildingIQ to control setpoints at the single zone units as well as exposing the proper data points for RTU-5. CSSI was able to resolve these issues by the end of August 2016.

BuildingIQ was able to perform several DR events in September that year and the entire summer of 2017 with complete control of the site.

In preparation for winter DR, CSSI was commissioned to implement additional programming changes that allowed BuildingIQ to take control of the zone temperature setpoints for each VAV box. This task was completed in October 2017. Controllability tests were performed to verify BuildingIQ’s writing capabilities at the VAV level.

As colder weather arrived in early January 2018, several winter DR events were executed with a proper response from all the pieces of equipment involved. The combination of an extensive renovation process with different BMS programming issues delayed the full DR implementation for several months until late summer 2016.

A deployment time frame of four weeks is expected on sites where atypical conditions like the ones described for USF Harbor Hall are not present.

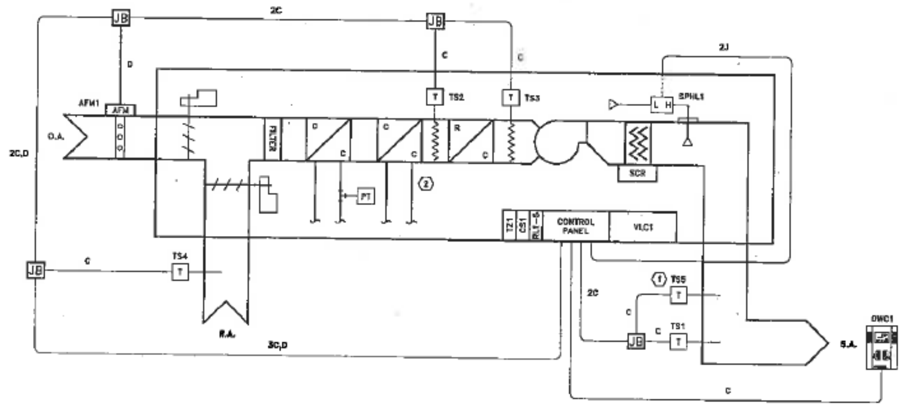

Figure 1. RTU Schematic.

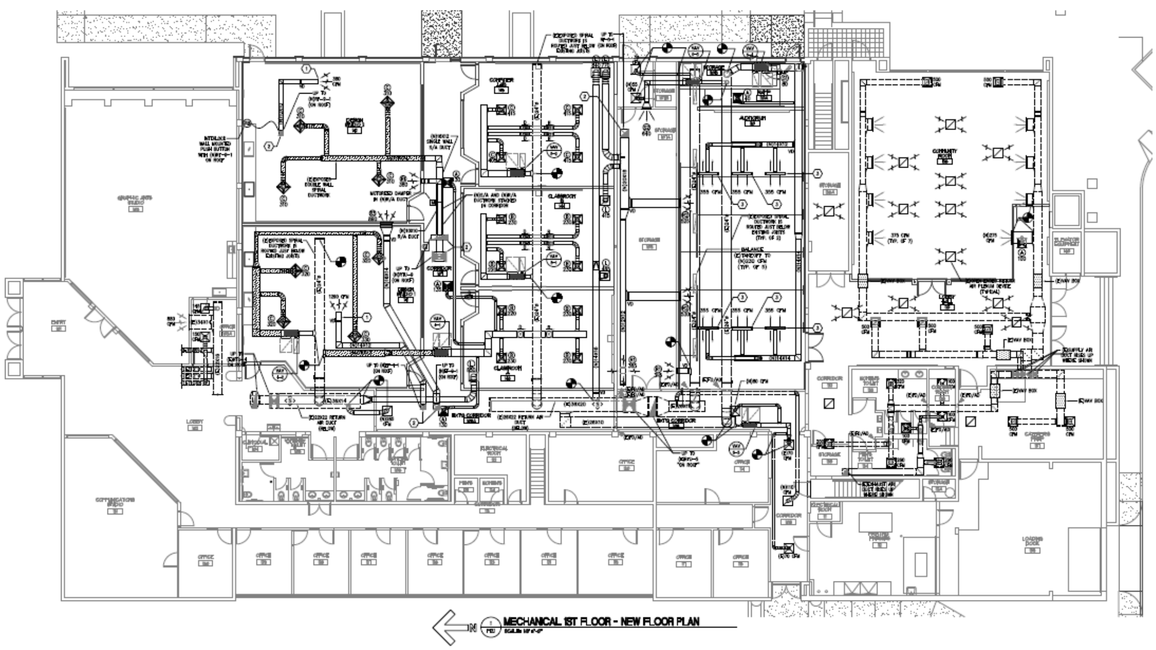

Figure 2. Mechanical Floor Plan.

Figure 3. USF Harbor Hall Exterior View.

IV. Summer DR Results

During summer DR, the supply air temperature and pressure setpoints as well as the zone temperature setpoints are modified to reduce the amount of work performed by compressors and fans. According to the BMS operation sequence, the RTUs will modulate compressor 1 and stage compressor 2 on an as-needed to maintain the cooling discharge setpoint of 52°F. The supply air temperature setpoint is ratcheted up beyond 52°F to decrease the compressor load while maintaining the supply air pressure at the minimum. For longer lasting events, relatively cooler air is provided to the zones for specific periods of time. These cooling periods are alternated between zones to avoid increasing the load in all units at the same time. Setpoints were also modulated during the hour following the event to slowly return the spaces to their pre-DR conditions and avoid a significant demand increase.

USF Harbor Hall participated in 25 events between August 2015 and October 2017. Events during 2015 were run with partial control of the building limiting the achievable demand reduction. Events were called at different times to determine the potential comfort impacts at different times of the day. Event duration was also modified to determine the length of time that the demand drop could have been maintained. **The**

average kW reduction was 25.5 kW which represents a drop of 27.3% with a maximum of 48 kW achieved on July 26th 2017 (Table 1). For this event, the DR settings aggressiveness was increased as the duration was extended to test the full demand shed capability in the middle of the summer. In early August, several units went through maintenance work which delayed the next event until late September. **None of the events were interrupted due to comfort complaints.** RTU-8 which supplies conditioned air to a large meeting room was not included in DR during the first and second week of June 2017 due to an ongoing event. The BuildingIQ DR system can be customized to exclude or modify the aggressiveness of the settings for specific zones.

Event Date	Average kW Reduction	Percentage Reduction	Start Time	Duration (min)	Comments
8/21/2015	6.1	8	15:00	30	Three units participated
8/24/2015	8.7	10.5	16:30	60	Three units participated
9/21/2015	4	6.5	14:00	60	Two units participated
9/22/2015	4.2	7.5	14:00	120	Two units participated
9/6/2016	20.6	22	14:00	60	One unit was overridden due to ongoing event
9/9/2016	28	27	14:00	60	All units responded to DR commands
9/12/2016	35.2	32	14:00	60	All units responded to DR commands
5/31/2017	36	44	15:00	30	All units responded to DR commands
6/1/2017	13.8	20	15:00	60	Communication issues during the first 30 min
6/8/2017	23.2	28	15:00	60	One unit did not participate due to ongoing event
6/14/2017	11.2	14	14:30	90	One unit did not participate due to ongoing event
6/15/2017	13.9	18	14:30	90	One unit did not participate due to ongoing event
6/21/2017	40.9	44	9:00	90	All units responded to DR commands
6/22/2017	30.5	37	19:30	90	All units responded to DR commands
6/23/2017	29.3	34	10:00	30	All units responded to DR commands
6/28/2017	33.2	33	10:00	30	All units responded to DR commands
6/29/2017	44.5	40	15:00	30	All units responded to DR commands
7/5/2017	35.5	38	15:00	30	All units responded to DR commands
7/6/2017	35	37	15:00	30	All units responded to DR commands
7/26/2017	48	49	14:00	240	All units responded to DR commands

9/28/2017	17.6	15	14:00	120	All units responded to DR commands
10/4/2017	17.3	21	14:00	120	All units responded to DR commands
10/5/2017	22.8	25	11:00	120	All units responded to DR commands
10/11/2017	40.2	35	14:00	120	All units responded to DR commands
10/12/2017	38.3	37	14:00	180	All units responded to DR commands
Average	25.52	27.3			

Table 1. Demand reduction during summer Demand Response events

V. Winter DR Results

During winter DR, the goal was to minimize electricity demand by reducing electric heating at the VAVs and RTU levels. Heating is present at the RTU (Hot Gas and Electric) and VAV (Electric). According to the BMS sequence of operations for the multi-zone units, heating mode will be enabled when any box requires heating, no other VAV box require cooling, and the outside air temperature is below 65F. The RTU will modulate its electric heat to maintain a supply air temperature setpoint of 70F. In the case of the single zone units, the RTU will modulate its electric heat to maintain the space temperature heating setpoints. BuildingIQ DR strategy modified the heating setpoints in each VAV box to turn off the electric reheats at that level. Additionally, the supply air temperature was adjusted to reduce electric heating and warm up the air exclusively with hot gas. Comfort levels were maintained as air was heated up at the RTU level. This configuration allowed the system to drop significant amounts of load without affecting comfort. Comfort complaints were not received during the events. Demand reduction of this magnitudes might not be achieved in buildings with electric VAV reheats as the only source of heating.

Eight events were performed in January 2018 during the early morning. **The average kW reduction was 53.6 which represents an average demand drop of 47.8%. The maximum demand reduction was achieved on January 18th with 70.5 kW (Table 2).** The building is schedule to start operating every weekday morning at 6:15 AM. Different event start times were tested to determine the effect of the DR events on the building warm-up at startup. Spaces were warmed up to comfortable levels regardless of the event start time due to the possibility of supplying warm air using hot gas. For longer events, the DR settings aggressiveness was reduced to allow some electric heating to be triggered for certain periods of time. VAV heating allowance was alternated between zones to avoid increasing the demand substantially. This strategy allowed the system to maintain DR events running for four hours and a half. After events ended, electric reheats were sequentially turned on during the following hour to avoid producing a demand peak by triggering reheat in all zones at the same time.

Event Date	Average kW Reduction	Percentage Reduction	Start Time	Duration (min)	Comments
1/5/2018	25.5	19	7:00	60	Three zones did not participate
1/15/2018	50.5	49	7:30	60	All units responded to DR commands
1/16/2018	64	60	6:30	60	All units responded to DR commands
1/17/2018	66.5	62	6:30	120	All units responded to DR commands
1/18/2018	70.5	52	7:00	240	All units responded to DR commands
1/19/2018	69.8	52	6:30	240	All units responded to DR commands
1/30/2018	40.6	44	7:30	300	All units responded to DR commands
1/31/2018	41	44	7:30	300	All units responded to DR commands
Average	53.6	47.8			

Table 2. Demand reduction during winter Demand Response events

VI. Summary

This report provides an outline of BuildingIQ's Demand Response technology and the results from summer and winter DR events performed at the University of South Florida Harbor Hall. BuildingIQ reduces HVAC electricity demand by dynamically and incrementally altering the supply air temperature, pressure, and zone temperature setpoints. BuildingIQ DR system is completely customizable which maximizes demand reduction while maintaining comfort in critical zones. The automated system is also monitored by BuildingIQ personnel who would implement adjustments to attend any comfort complaints received from the building during and after the event.

Thirty-two DR events were conducted in the building in a two year and a half period. Average demand reductions of 27.3% for summer and 47.8% for winter events show the potential of BuildingIQ DR strategy to reduce electricity demand in different seasons, times of the day and different event lengths.

Seasonality - The large difference in demand reduction potential between seasons is mainly due to the power demand of VAV's electric reheats. For example, VAVs associated with RTU-4 and 5 add up to a reheat capacity of 65.5 kW. That represents more than half of the peak demand for a typical summer day. Winter peak demand is significantly larger during winter than summer allowing the BuildingIQ system to drastically reduce the demand by minimizing reheats at the VAV boxes.

Comfort Factors - Based on the results from this project, the potential for shedding load in this region would mainly depend on comfort constrains from tenants and equipment characteristics. Educating tenants about DR activities could lead to a larger comfort tolerance. In sites such as hospitals, laboratories, and event centers where comfort requirements are strict, demand reduction would be minimal. Increasing aggressiveness on unoccupied areas would maximize the demand reduction.

Equipment - In terms of equipment configuration, BuildingIQ could reduce the load between 15 to 25% from mechanical cooling either if the system has compressor units or a chiller plant during summertime. Sites with chiller plants have a larger potential to reduce demand when resets at the air handler level are coupled with supply water temperature at chiller level. On the air distribution side, fans with variable frequency drives are more suitable for load shed as the BuildingIQ DR system would reduce fan speed accordingly. For winter DR, instead of a reliance on electric reheats, the use of multiple heating sources could maximize the demand reduction without affecting comfort. In USF Harbor Hall, this component was the main factor that allowed demand reductions of more than 50%. The BuildingIQ system is flexible enough to work with different types of HVAC configuration. However, digital controls are an important factor to be able to reduce the load while maintaining comfort. Reliable temperature information from the zones would allow the system to properly reset the supply air temperature and pressure setpoints during summer DR. Control of the zone temperatures would allow the system to reduce electric heating at the VAV level. In a commercial building with only electric reheats, as it is typical in Central Florida, demand could be decreased between 20 and 30% by minimizing reheats at the VAV boxes while maintaining certain levels of comfort.

ELECTRIC POWER RESEARCH INSTITUTE

Variable Capacity Heat Pump Applications

Elimination of Backup Electric Resistance Heat

3002014920

Variable Capacity Heat Pump Applications

Elimination of Backup Electric Resistance Heat

3002014920

Technical Update, November 2018

EPRI Project Manager

W. Hunt

ELECTRIC POWER RESEARCH INSTITUTE
3420 Hillview Avenue, Palo Alto, California 94304-1338 • PO Box 10412, Palo Alto, California 94303-0813 • USA
800.313.3774 • 650.855.2121 • askepri@epri.com • www.epri.com

DISCLAIMER OF WARRANTIES AND LIMITATION OF LIABILITIES

THE ELECTRIC POWER RESEARCH INSTITUTE (EPRI) PREPARED THIS REPORT.

This is an EPRI Technical Update report. A Technical Update report is intended as an informal report of continuing research, a meeting, or a topical study. It is not a final EPRI technical report.

NOTE

For further information about EPRI, call the EPRI Customer Assistance Center at 800.313.3774 or e-mail askepri@epri.com.

ACKNOWLEDGMENTS

The Electric Power Research Institute (EPRI) prepared this report.

Principal Investigator
W. Hunt

This report describes research sponsored by EPRI.

EPRI would like to acknowledge the continuous support of George Gurlaskie from Duke Energy in conducting this research project.

This publication is a corporate document that should be cited in the literature in the following manner:

Variable Capacity Heat Pump Applications: Elimination of Backup Electric Resistance Heat. EPRI, Palo Alto, CA: 2018. 3002014920.

ABSTRACT

This study builds upon previous work in exploring the ability of variable capacity heat pumps to eliminate backup electric heat in Central Florida residences. This study consisted of examining two unique variable capacity heat pump product categories: high heating systems and cost competitive products. Two variable capacity heat pump field sites were included in this effort: a high heating system in Ocala, FL and a cost competitive product in Clearwater, FL. Ocala is representative of the coldest territory in Central Florida, while Clearwater is representative of the mildest climate during a typical winter season. The performance of the two variable capacity heat pumps was compared to previously obtained baseline data at each site. The utility and customer effectiveness of a representative variable capacity heat pump were examined for multiple cases for Central Florida.

Keywords
Variable Capacity
Heat Pumps
HVAC

ELECTRIC POWER RESEARCH INSTITUTE

EXECUTIVE SUMMARY

Deliverable Number: 3002014920

Product Type: Technical Update

Product Title: Variable Capacity Heat Pump Applications: Elimination of Backup Electric Resistance Heat

PRIMARY AUDIENCE: Emerging Technology Researchers; Utility Program Implementers

KEY RESEARCH QUESTION

Duke Energy has identified backup electric heat in heat pumps as a primary contributor to winter peak events in Central Florida. Variable capacity heat pumps (VCHPs) can potentially alleviate this issue through their ability to provide increased heating capacity at lower outdoor temperatures when compared to traditional, fixed-speed heat pumps. In addition, VCHPs provide an energy efficiency resource, as they offer best-in-class efficiency in today's residential HVAC market. Multiple categories of VCHPs are common in today's market including high heating output products and cost competitive products. Each VCHP product would have a unique impact on energy efficiency, demand reduction, and overall effectiveness for Central Florida residences. This study aimed to examine unique VCHP products in the field and to explore the potential effectiveness of VCHPs for Duke Energy and their customers in Central Florida.

RESEARCH OVERVIEW

This study builds upon a previous effort in exploring the ability of VCHPs to eliminate backup electric heat in Central Florida residences. The previous study examined a VCHP product in two Orlando residences. The VCHP for one Orlando site was oversized for space cooling and demonstrated an ability to eliminate backup heat, while the VCHP at the other Orlando site was right-sized for space cooling and demonstrated significant reduction but not elimination of backup electric heat. Further details and findings of the previous study (Phase I) can be found within the EPRI Technical Update 3002004964. This study (Phase II) explored two additional VCHP applications for Central Florida: a high heating output VCHP in Duke's northern territory (Ocala) and a cost competitive VCHP in Duke's coastal territory (Clearwater). This study consisted of VCHP field monitoring for multiple winter seasons and examined the energy and demand impact of the selected VCHPs and applications. The cumulative findings across Phase I and II were utilized to explore the utility and customer effectiveness of VCHPs for Central Florida residences.

KEY FINDINGS

- Each of the leading U.S. HVAC manufacturers produces a VCHP product. Available VCHPs consist of rated seasonal cooling efficiencies from approximately 15 to over 20 SEER, and rated heating efficiencies from approximately 10 to 13 HSPF. In the marketplace, there are at least three available VCHPs which offer nominal heating capacity at 17°F and could be considered high heating output systems. In addition, there are at least four available VCHPs which could be considered cost competitive systems.
- During Phase II data collection, all three sites that were specified to eliminate backup heat (oversized Orlando, Clearwater, and Ocala) demonstrated an ability to sufficiently heat their residence during cold outdoor conditions for the territory with minimal or no backup electric heat.

ELECTRIC POWER RESEARCH INSTITUTE

EXECUTIVE SUMMARY

- During the coldest period of data collection for this study, the oversized Orlando and Ocala VCHP sites demonstrated peak demand reduction of 8.5 kW at 34°F and 5.8 kW at 26°F, respectively.
- For cooling operation, the Clearwater VCHP rated at 20 SEER demonstrated energy savings of approximately 25% over the existing baseline 13 SEER system.
- For Phase II data collection, the three sites that were specified to eliminate backup heat (oversized Orlando, Clearwater, and Ocala) demonstrated an average HVAC winter peak demand comparable to the average HVAC summer peak demand. Outdoor conditions and weather patterns during the Phase II winter data collection were milder than the previous winter peak conditions of 2010.
- Equipment cost is the primary variable impacting the increased cost associated with VCHPs. Based on potential Central Florida applications for eliminating backup heat, the first cost difference from baseline to VCHP is approximately $2,000 to $3,250 using wholesale pricing or $3,000 to $4,875 using estimated retail pricing. The lower price differentials would be representative of cost competitive VCHPs, while the upper price differentials would be representative of oversized, high heating VCHPs.
- Based on the collective field results of Phase I and II and additional energy modeling, the implementation of a VCHP specified to eliminate backup heat in Central Florida could achieve 2,000 to 3,000 kWh annual energy savings, 0 to 0.5 kW cooling peak demand reduction, and 2.5 to 5.0 kW heating peak demand reduction. The specific performance of a VCHP depends upon equipment selection, residential application, and location in Central Florida.
- Utilizing cost differential, energy reduction, and demand reduction values for representative VCHP applications specified to eliminate backup electric heat, utility and customer effectiveness was explored using standard utility tests and assumptions. Across the examined VCHP implementation scenarios, the total resource cost (TRC) test yielded benefit-to-cost ratios ranging from 0.5 to 1.8, and the participant test benefit-to-cost ratios varied from 0.4 to 1.6.
- From a TRC and participant perspective, the implementation of VCHPs was generally most effective for applications with higher annual HVAC energy savings and for cases in which the VCHP sizing was similar to baseline. Annual HVAC energy savings would vary based on VCHP equipment (e.g. 4-ton, 18 SEER) and thermal load characteristics (e.g. 2,000 ft² residence in Orlando climate). TRC ratios near or above 1.0 were observed for both cost competitive and high heating VCHPs which were sized similar to baseline. The implementation of VCHPs was generally least effective for applications with lower annual energy savings and for cases in which oversizing the VCHP was required to eliminate backup heat. The reduced effectiveness of oversized VCHPs is primarily due to the increased cost of stepping up to a higher nominal size for an already premium product.

WHY THIS MATTERS

VCHPs offer electric utilities a new resource for energy efficiency, demand reduction, and demand control in residential applications. Today, variable capacity heat pumps occupy a small portion of the HVAC market, but steady growth in market share is expected in the coming years. Understanding the current benefits of implementing variable capacity technology and the future impact of wide-spread variable capacity systems are prime areas of research for electric utilities.

ELECTRIC POWER RESEARCH INSTITUTE

EXECUTIVE SUMMARY

HOW TO APPLY RESULTS

The content of this report is applicable to the residential sector and to ducted, central VCHPs. In this report, the background content of utilizing VCHPs for backup heat elimination is applicable to all territories, but the detailed VCHP performance analysis in this report is primarily applicable to the southern portion of the Southeastern U.S. The findings could be applied to continued research on VCHP applications and the development of utility programs in Central Florida.

LEARNING AND ENGAGEMENT OPPORTUNITIES

This study on the *Elimination of Backup Electric Resistance Heat* is part of a larger project, *Variable Capacity Heat Pump Applications*. Five utilities are participating in this collaborative project. Each utility is exploring a unique application and VCHP equipment type. Applications of note include school classrooms and hot-dry climates, and VCHP equipment types including ducted, central systems and ducted, mini-splits.

EPRI CONTACTS: Walt Hunt; whunt@epri.com

PROGRAM: Program 170: Energy Efficiency and Demand Response

CONTENTS

LIST OF FIGURES

LIST OF TABLES

1
BACKGROUND

Introduction

Duke Energy has identified backup electric heat in heat pumps as a primary contributor to winter peak events in Central Florida. Variable capacity heat pumps (VCHPs) can potentially alleviate this issue through their ability to provide increased heating capacity at lower outdoor temperatures when compared to traditional, fixed-speed heat pumps. In addition, VCHPs provide an energy efficiency resource, as they offer best-in-class efficiency in today's residential HVAC market. This study examines the potential effectiveness of VCHPs for Central Florida in the *ducted, split* and *whole-home* or *central* configuration.

This study builds upon a previous effort in exploring the ability of VCHPs to eliminate backup electric heat in Central Florida residences [1]. The previous study examined a VCHP product in two Orlando residences. The VCHP at one Orlando site was oversized for space cooling and demonstrated an ability to eliminate backup heat, while the VCHP at the other Orlando site was right-sized for space cooling and demonstrated significant reduction but not elimination of backup electric heat.

The continued research effort described in this report explored two additional VCHP applications for Central Florida: a high heating output VCHP in Duke-Florida's northern territory and a cost competitive VCHP in Duke's coastal territory. The study consisted of VCHP field monitoring for multiple winters and examined the energy and demand impact of the selected VCHPs and applications. The cumulative findings from the two research efforts were utilized to explore the utility and customer effectiveness of VCHPs for Central Florida residences.

Categories of Available VCHPs

Multiple categories of ducted, split VCHPs are common in today's market including high heating output products and cost competitive products. Each HVAC manufacturer has developed a unique product with unique attributes: cooling efficiency, heating efficiency, low temperature heating performance, and incremental cost. Each VCHP product would have a unique impact on energy efficiency, demand reduction, and overall effectiveness for Central Florida customers.

In this report, a "high heating output" VCHP is a product which can supply nominal or rated heating capacity at 17°F. Standard HVAC ratings for heat pumps are provided at 47°F (the rating condition) and 17°F by the Air-Conditioning, Heating, and Refrigeration Institute (AHRI) [2]. As an example, a VCHP which has a standard rating of approximately 24,000 Btu/h of heating at 47°F and approximately 24,000 Btu/h at 17°F would be considered "high heating output".

Figure 1-1 illustrates the general heating output curve for multiple VCHP types and a representative baseline heat pump. For a baseline heat pump, the heating capacity available at 17°F is ~65% of the rated or available capacity at 47°F. A portion of the VCHP products in the market have "baseline" low temperature heating performance. For a high heating output VCHP, the heating capacity at 17°F would be ~100% of the rated capacity at 47°F. An "oversized, high heating output" VCHP refers to a system which is both "high heating" and "oversized" (increased nominal size) from the perspective of the cooling load. Considerations for oversizing a VCHP were a primary point of discussion in the previous VCHP assessment for backup heat elimination [1, Chapter 1: *Sizing of Residential HVAC Equipment*]. Oversized VCHPs may be necessary to eliminate backup electric heat in a percentage of Central Florida residences. In general, VCHPs offer a level of improved heating performance at 17°F when compared to baseline heat pumps. In Figure 1-1, the "Standard VCHP" curve is representative of multiple VCHP products which offer ~80% of rated heating capacity at 17°F. Products offering "Standard VCHP" heating performance may fall into either the "high-end" or "cost competitive" product category for a given manufacturer.

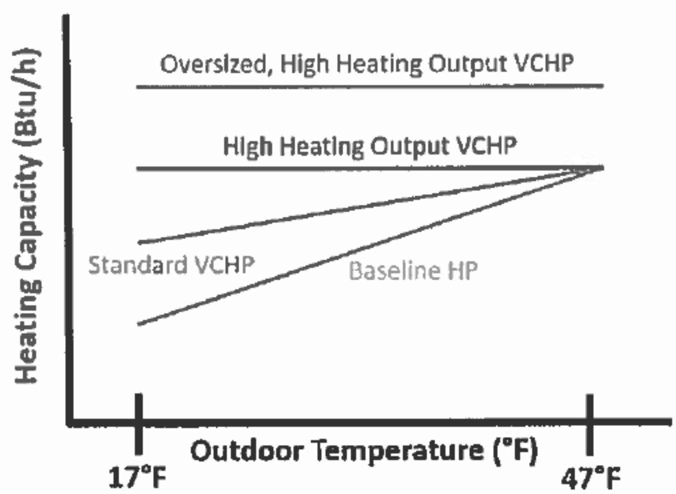

Figure 1-1
Heating Comparison of Baseline HP and Categories of VCHPs

A "cost competitive" VCHP refers to a product which is produced by a manufacturer to be a more financially-viable option for customers considering variable capacity equipment. A common trend in the market is HVAC manufacturers producing two variable capacity products: a high-end, higher cost product and a cost competitive product. The "high-end, higher cost" category includes the VCHP attributes of high heating output and high efficiency. "Cost competitive" VCHP products would aim to have an intermediate level of efficiency and cost, between the "high-end" VCHPs and baseline equipment. For example, a manufacturer may produce a "high-end" VCHP with SEER of 20 and a cost competitive VCHP with SEER of 18. Currently, there are VCHP products in the market which could be considered both "cost competitive" and "high heating output".

Each of the leading U.S. HVAC manufacturers produces a VCHP product for the residential market. Table 1-1 provides a sample list of available VCHP products and indicated whether the product could be considered "cost competitive" or "high heating output". In the market, there are at least three available VCHPs which offer nominal heating capacity at 17°F and could be considered high heating output systems. In addition, there are at least four available VCHPs which could be considered cost competitive systems. Available VCHPs consist of rated seasonal cooling efficiencies from approximately 15 to over 20 SEER, and rated heating efficiencies from approximately 10 to 13 HSPF.

Table 1-1
Sample List of Available VCHP Products

Manufacturer	Series	High Heating Output Design[1]	Standard Heating Design[2]	Cost Competitive
Carrier	Greenspeed	✓		
	Infinity 18VS			✓
Daikin	DZ20VC		✓	
	DZ18VC			✓
Lennox	XP25			
	XP20			✓
Mitsubishi	P-Series H2i	✓		
Rheem	RP20	✓		
Trane	XV20i		✓	
	XV18		✓	✓

1. High Heating Output Design refers to VCHPs capable of providing ~100% nominal capacity at 17°F.
2. Standard Heating Design refers to VCHPS capable of providing ~80% of nominal capacity at 17°F.

Project Overview

The research direction for this project was to: expand upon the previous investigation of VCHPs for backup heat elimination (completed during Phase I), consider other unique VCHP products potentially applicable to the Central Florida climate (Phase II), and examine the effectiveness of residential VCHPs for the utility and it's customers. Table 1-2 describes the four VCHP field sites utilized across Phase I and II. In Phase I, a VCHP product was installed at two residences in Orlando. The VCHP system at one field site was sized similar to the baseline system, while the VCHP system at the other was oversized from a cooling perspective. In Phase II, a cost competitive VCHP was examined in a Central Florida's milder winter territory (Clearwater) and a high heating output VCHP was examined in Central Florida's coldest territory (Ocala). Within this report, field data and site characteristics for all four sites were utilized to examine the effectiveness of VCHPs in eliminating backup electric heat for Central Florida residences.

Table 1-2
Overview of Project Field Evaluations

Research Study	Site	VCHP Field Site Description	Location
Phase I	1	Right-Sized for Cooling (Same size as Baseline)	Orlando, FL
	2	Oversized for Cooling (Oversized from Baseline)	Orlando, FL
Phase II	3	Cost Competitive Product in Milder Territory	Clearwater, FL
	4	High Heating Product in Colder Territory	Ocala, FL

2
VCHP FIELD EVALUATION

This chapter contains details of the VCHP field evaluation including: the VCHP equipment selection process, VCHP equipment examined at the selected field sites, field site instrumentation, field heating performance analysis, field cooling performance analysis, and an investigation of the annual power demand profile of VCHPs for Central Florida.

VCHP Equipment Selection Process

Residential HVAC equipment is sized in accordance with cooling and heating load calculations determined through the ACCA *Manual J: Residential Load Calculation* [3]. Table 2-1 provides the design heating and cooling outdoor temperatures for the selected Central Florida cities from Manual J. The low outdoor temperatures during the 2010 winter peak for Central Florida is also listed in the table. For Central Florida, the norm has been to size a heat pump based on the cooling load. With baseline equipment in Central Florida, this allows for appropriate cycling and dehumidification to occur in cooling operation, but often results in significant backup electric heat usage during peak heating conditions. The emergence of variable capacity technology in VCHPs allows for flexibility in equipment sizing. Equipment sizing with variable capacity heat pumps for Central Florida was discussed and investigated in detail in the previous effort [1].

Table 2-1
Design Outdoor Temperatures for Examined Central Florida Locations [4]

City	Heating Season		Cooling Season
	Design Outdoor Temperature (°F)	2010 Actual Low Outdoor Temperature (°F)	Design Outdoor Temperature (°F)
Orlando, FL	42	28	93
Ocala, FL	34	17	93
Clearwater, FL	47	30	93

Table 2-2 provides the design cooling load and design heating load based on Manual J load calculations for each of four field sites. In addition, the table provides an estimated peak heating load for each field site. In order for a VCHP to eliminate or minimize backup electric heat, a heat pump should be able to supply heating capacity at or above the "peak" heating load at the corresponding outdoor temperature. In practice, a VCHP can be implemented to eliminate backup electric heat based on Manual J load calculations and a combination of manufacturer product data and AHRI ratings. The general VCHP type (i.e. oversized high heating, high heating or standard VCHP) which should be considered for a site can be determined by considering the difference between the design cooling load and peak heating load. If the cooling design load and peak heating load are similar, then a high heating output VCHP could potentially be utilized to eliminate backup electric heat. If the design cooling load is greater than the peak heating load, then a standard heating VCHP could potentially be utilized to eliminate backup electric heat. If the peak heating load is greater than the design cooling load, then an oversized, high heating VCHP could potentially be utilized to eliminate backup electric heat. As shown in Table 2-2, all three situations were observed throughout the selected Central Florida sites. In the milder territory of Clearwater, a "standard" heating VCHP could be utilized. In the coldest territory of Ocala, a high heating VCHP could be utilized. For both Orlando sites, an oversized high heating VCHP was necessary to eliminate backup electric heat.

Table 2-2
VCHP Designs for Field Sites to Eliminate Backup Heat

Site	Design Load		Estimated Peak Heating Load (Btu/h)	Cooling Load vs. Peak Heating Load	VCHP Type Required to Minimize Backup Heat
	Cooling (Btu/h)	Heating (Btu/h)			
1 (ORL)	38,500	32,500	45,000	Peak Heating Load greater by 6,500 Btu/h	Oversized High Heating Output VCHP
2 (ORL)	51,500	45,000	57,000	Peak Heating Load greater by 5,500 Btu/h	Oversized High Heating Output VCHP
3 (Clear)	35,500	17,000	26,000	Cooling Load greater by 9,500 Btu/h	Standard Heating VCHP
4 (Ocala)	39,000	28,500	39,000	Identical or Similar	High Heating Output VCHP

1. High Heating Output Design refers to VCHPs capable of providing ~100% nominal capacity at 17°F.
2. Standard Heating Design refers to VCHPS capable of providing ~80% of nominal capacity at 17°F.

Details of VCHPs at Field Sites

Table 2-3 provides a summary of the VCHP equipment examined at each of the four field sites in Central Florida. Due to the progression of research through Phase I and II, three of the four field sites were implemented to eliminate backup electric heat based on equipment selection and equipment sizing. Three unique VCHP products were included within the field assessment. At three of the field sites, a high heating VCHP which could offer nominal capacity at 17°F was utilized. At one field site, a VCHP intended to be representative of a cost competitive product was examined. During the equipment selection process, the manufacturer of the labeled "cost competitive" product only offered a single VCHP system. Based on industry discussions at that time, this product was intended to fall into the "cost competitive" category. In the following years, the manufacturer produced a second VCHP product with an intermediate level of efficiency (e.g. 18 SEER), which may better represent a "cost competitive" solution in the current market.

Table 2-3
VCHP Products Examined at Field Sites

Site	Implemented to Eliminate Backup Heat	High Heating VCHP[1]	Cost Competitive, Standard Heating VCHP[2]	SEER	HSPF	Manufacturer and Series
1 (ORL)		✓		19.0	10.5	Carrier Greenspeed
2 (ORL)	✓	✓		18.0	12.0	Carrier Greenspeed
3 (Clear)	✓		✓	20.0	10.0	Daikin DZ20VC
4 (Ocala)	✓	✓		15.3	11.0	Mitsubishi P-Series H2i

1. High Heating Output Design refers to VCHPs capable of providing ~100% nominal capacity at 17°F.
2. Standard Heating Design VCHP refers to VCHPS capable of providing ~80% of nominal capacity at 17°F.

Table 2-4 provides a comparison of the rated seasonal cooling and heating efficiency of the baseline and VCHP equipment at each field site. Rated cooling efficiency is represented by the Seasonal Energy Efficiency Ratio (SEER), while rated heating efficiency is represented by Heating Seasonal Performance Factor (HSPF). SEER and HSPF are determined in accordance with AHRI Standard 210/240, which governs residential heat pumps. Baseline equipment with SEER of 13 and HSPFs of 7.7 to 8.2 is representative of existing heat pumps in Central Florida. The VCHP equipment ranged from 15.3 to 20.0 SEER and from 10.0 to 12.0 HSPF. The efficiency range of the considered VCHP equipment generally represents the range of VCHP efficiency available in the market. VCHPs with higher SEER and HSPF are expected to have higher annual energy savings for cooling and heating, respectively.

Table 2-4
Baseline and VCHP Rated Efficiency Comparison at Project Field Sites

Site	SEER (Btu/Wh)		HSPF (Btu/Wh)	
	Baseline	VCHP	Baseline	VCHP
1 (ORL)	13.0	19.0	7.7	10.5
2 (ORL)	13.0	18.0	8.2	12.0
3 (Clear)	13.0	20.0	7.7	10.0
4 (Ocala)	13.0	15.3	8.0	11.0

Table 2-5 provides the nominal equipment and backup electric heat sizing for the baseline and VCHP systems at each of the four field sites. Three of the VCHPs were sized similar to the existing baseline heat pump, while one of the VCHP field sites was oversized from the perspective of the cooling load. For two of the VCHPs, backup electric heat was able to be reduced in nominal size, and backup electric heat was not installed with one of the VCHP field sites. With VCHPs, backup electric heat may be necessary to offset the defrost operation or to provide a means of emergency heating for the heat pump system. The VCHP product at Field

Sites 1, 2, and 3 utilized a reverse cycle defrost, which would blow cold air into the occupied space if electric heat were not installed. The VCHP at Field Site 4 did not utilize reverse cycle defrost, so cold supply air was not the occupied space during system defrost. The ability to significantly reduce backup electric heat at a site (e.g. Site 2 and 4) offers a level of "guaranteed" peak demand reduction with VCHP equipment based on the maximum power demand of the heat pump and backup heat. Additionally, demand savings can be "guaranteed" utilizing the unit settings of VCHPs. The importance of utilizing unit settings to allow for the elimination of backup heat was a key take-away from the previous study [1, Chapter 3: *Backup Heat Usage Comparison*], as backup electric heat may be triggered in VCHPs with increases to the indoor temperature setpoint by the homeowner or through a schedule.

Table 2-5
Baseline and VCHP Equipment Sizing Comparison at Selected Field Sites

Site	Size (tons)		Electric Heat Size (kW)	
	Baseline	VCHP	Baseline	VCHP
1 (ORL)	3	3	10	8
2 (ORL)	4	5	10	5
3 (Clear)	3	3	5	5
4 (Ocala)	3.5	3.5	8	-

Figure 2-1 shows the outdoor units of the VCHPs at the field sites in Clearwater and Ocala. At each of the sites, the ducted indoor unit was housed in attic space above the garage. Ductwork supplied the conditioned air throughout each residence. During the installation and commissioning process (2015), ductwork modifications were required at the Clearwater field site, while minimal duct modifications were performed at the Ocala field site. At the Clearwater site, duct modifications improved duct leakage from 45% to 14%. The condition of the ductwork during 2009 to 2010 baseline data collection is unknown, and thus adjustments to data comparisons were not performed. The duct modifications improved the efficiency of the VCHP at Field Site 3 by ~25%. Details of the Orlando sites are contained within the *HVAC Equipment* section in Chapter 2 of the previous study [1].

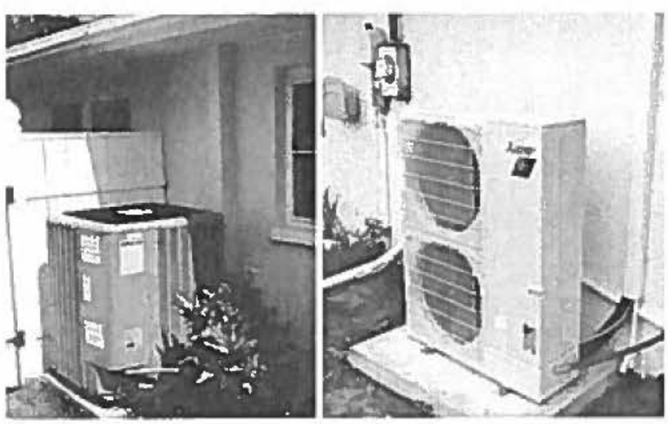

Figure 2-1
VCHP Products at Clearwater and Ocala Field Sites

Field Instrumentation

Table 2-6 provides the instrumentation package deployed at each of the selected VCHP field sites. The field data collection included outdoor unit power consumption, indoor unit power consumption, outdoor temperature and humidity, indoor temperature and humidity, and supply air temperature and humidity. The field data collected allowed for an investigation of VCHP performance for heating efficiency, backup heat usage, and cooling efficiency. All data collection for the VCHP equipment was conducted using this monitoring package and as part of this research effort. The baseline heat pump data at each site collected in 2009 and 2010 was supplied by the utility to support this project. Further details of the field instrumentation and experimental setup can be found in the *Data Acquisition* section in Chapter 2 of the previous study [1].

Table 2-6
Summary of Instrumentation at Each Field Site

Measurement	Instrumentation	Accuracy
Outdoor Temperature and Humidity	Dwyer RHP - 2011	±0.36°F; ±2% RH
Indoor Temperature and Humidity	BAPI Room Sensor	±0.36°F; ±2% RH
Supply Air Temperature and Humidity	BAPI Duct Sensor	±0.36°F; ±2% RH
Indoor Unit (Blower + Electric Heat) Power	WattNode	0.5% nominal
Outdoor Unit (Heat Pump) Power		

Heating Performance

To investigate the ability of the deployed VCHPs to eliminate backup electric heat, the coldest day of data collection for Phase II was considered for each field location. Figure 2-2, Figure 2-3, and Figure 2-4 illustrate the daily HVAC power consumption profile for the coldest day for each VCHP implemented to eliminate backup electric heat (i.e. Sites 2, 3, and 4). Backup electric heat usage can be observed through spikes in the HVAC power profile or when power demand is above nominal residential heat pump levels (e.g. 3 – 5 kW). For each of the VCHP profiles, a comparable cold day of baseline heat pump data was placed for comparison on each figure. Figure 2-2 shows the oversized, high heating output VCHP in Orlando, while Figure 2-3 and Figure 2-4 provide a comparison for the cost competitive VCHP in Clearwater and the high heating output VCHP in Ocala, respectively. The data presented in the three figures is for 15-minute average power data.

As highlighted in previous study, the winter peak demand hours for Central Florida are approximately 7 A.M. and 8 A.M., which generally corresponds with the coldest daily outdoor temperature. Figure 2-2 and Figure 2-4 clearly illustrate the substantial power demand of the baseline HVAC equipment during those peak demand hours. During the baseline data collection of Field Site 3 (Figure 2-3), the homeowner was enrolled in the utility's load shed program, and thus their HVAC power peak was regularly shifted to later in the day during colder weather. As seen in all three figures, the VCHP equipment operated with minimal to no backup electric heat usage. This field data supports the cold weather heating ability of VCHPs and the implementation strategy for eliminating backup electric in these Central Florida residences.

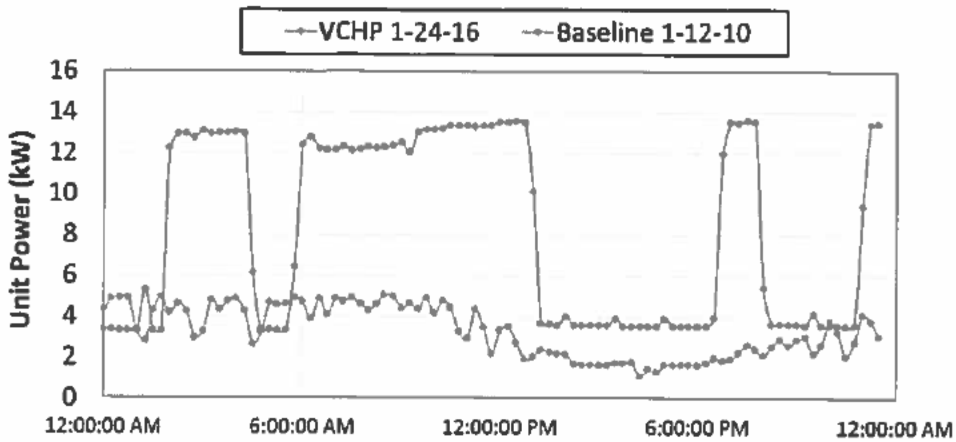

Figure 2-2
Site 2 – VCHP vs. Baseline Demand Profile for Coldest Day of Phase II

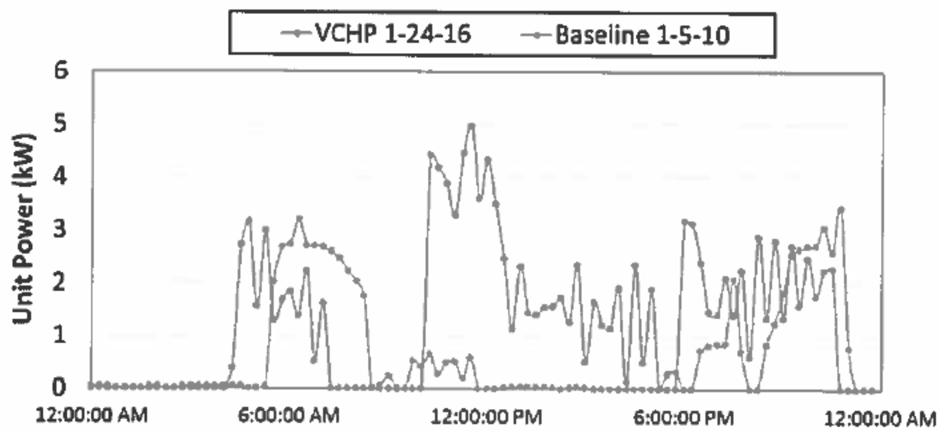

Figure 2-3
Site 3 – VCHP vs. Baseline Demand Profile for Coldest Day of Phase II

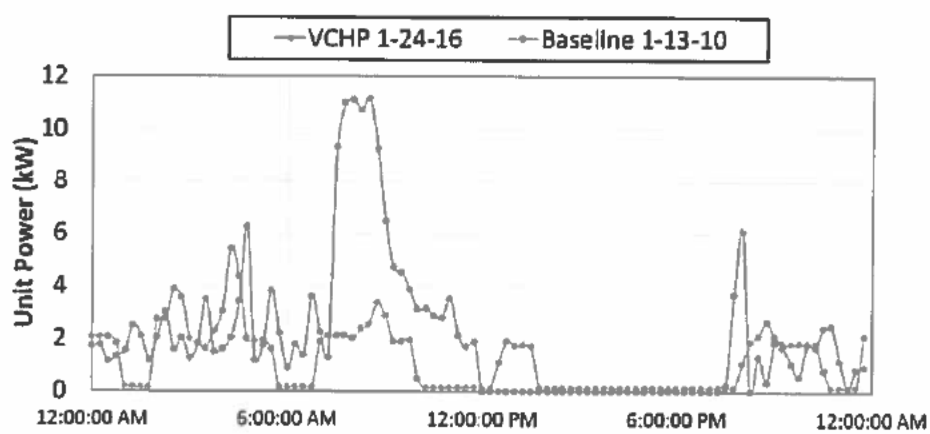

Figure 2-4
Site 4 – VCHP vs. Baseline Demand Profile for Coldest Day of Phase II

Table 2-7 provides a numerical summary of the HVAC peak demand comparison for the coldest day of Phase II data collection. The data presented in Table 2-7 corresponds to the same days and power profiles illustrated in Figure 2-2, Figure 2-3, and Figure 2-4. The data presented in Table 2-7 is for the maximum HVAC peak demand over the 24-hour day under consideration. For Sites 2 and 4 (where the VCHP was implemented to eliminate backup heat and where the sites were not enrolled in the utility load shed program), the peak power demand savings was 63% and 52%, respectively.

Table 2-7
Peak Demand Comparison for Coldest Day of Phase II Data Collection

	Site 1 (ORL)	Site 2 (ORL)	Site 3 (CLEAR)	Site 4 (OCALA)
Similar Day Baseline Peak Demand (kW)	12.2	13.6	5.0	11.2
VCHP Peak Demand on 1-24-16 (kW)	11.0	5.1	3.4	5.4
Demand Reduction (kW)	1.2	8.5	1.6	5.8
Percent Demand Reduction	10%	63%	32%	52%

Minimum Outdoor Temperature on 1/24/16 in Florida:
39°F Clearwater, 34°F Orlando, 26°F Ocala

As described in the *Backup Heat Usage Comparison* section of Chapter 3 for the previous study, defrost operation may result in regular but limited backup electric heat usage [1]. The VCHP at Field Site 3 operated in similar manner during defrost as the VCHP examined in Phase I. Figure 2-5 illustrates a daily profile of VCHP Site 3 for power, indoor temperature, and outdoor temperature. As seen in the figure, defrost operation occurs routinely with outdoor temperatures below 40°F. In this window, defrost cycles are occurring regularly every ~40 minutes for a duration of ~3.5 minutes. The backup electric heat (5 kW) is engaged during defrost operation.

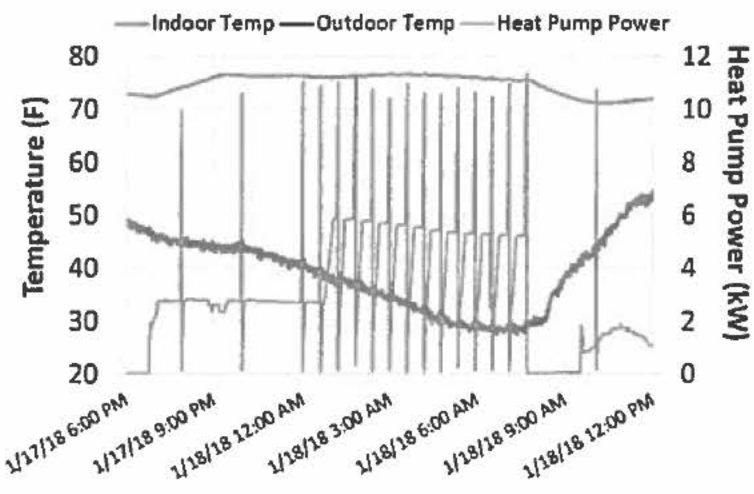

Figure 2-5
Defrost Frequency on Cold Day at VCHP Site 3 (1-Minute Average Data)

In Phase I, the VCHPs under consideration demonstrated "maximum operation" in response to an indoor setpoint temperature increase. For instance, increasing the indoor temperature setpoint from 68°F to 72°F [1]. For the Phase I VCHP, this resulted in "maximum" heat pump operation and "maximum" backup heat operation. A similar occurrence was observed at VCHP Field Site 4, as the home occupants frequently adjusted the indoor temperature setpoint of the VCHP. Figure 2-6 demonstrates an occurrence of this effect at Field Site 4. At approximately 10 P.M. on January 17th, 2018 the indoor temperature setpoint was adjusted from approximately 70°F to 75°F, which triggered "maximum operation" and a power demand of ~6 kW for the VCHP. At the coldest point of the shown timeframe (6 A.M. on January 18th, 2018) with an outdoor temperature of ~25°F, the VCHP operates at part-load operation with a demand of ~2 kW.

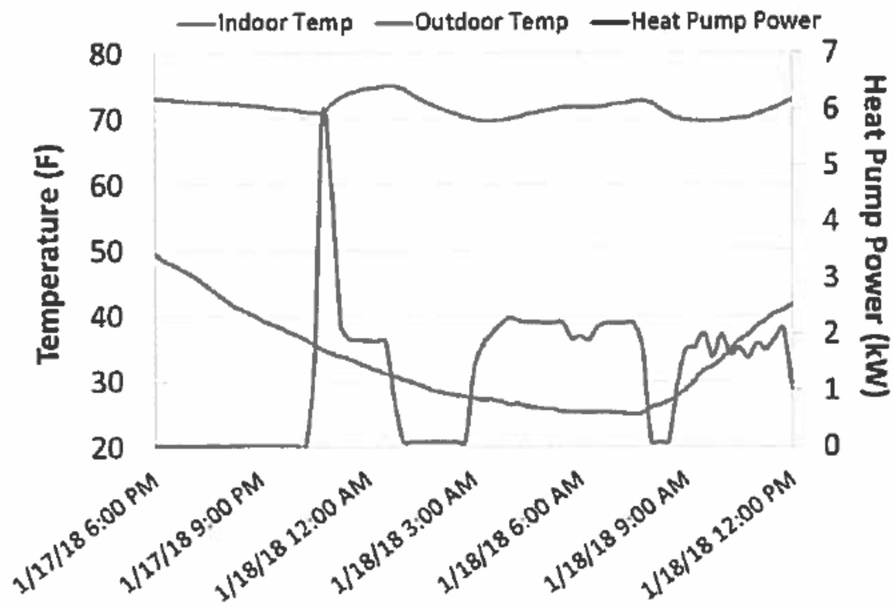

Figure 2-6
Impact of Setpoint Adjustment on VCHP Operation – Field Site 4

Table 2-8 provides an HVAC energy consumption comparison for the VCHP at Field Sites 3 and 4 for the coldest day of Phase II data collection. For each site, a comparable day of weather was selected from baseline data for comparison. As discussed, ductwork modifications were performed at Field Site 3, and thus differences in the distribution system between the baseline and VCHP data collection may impact the energy consumption comparison. The rated equipment heating efficiency at the sites from baseline to VCHP changed from 7.7 to 10.0 and 8.0 to 11.0 for Sites 3 and 4, respectively. Heating energy savings for this cold day were 47% and 41% for Field Sites 3 and 4, respectively. The potential energy savings of VCHPs for heating operation can be attributed in part to their increased designed heating efficiency (e.g. increased HSPF or COP) and in part to their decreased usage of inefficient, backup electric heat through the improved heating output of VCHPs at low outdoor temperatures.

Table 2-8
Energy Consumption Comparison for Coldest Day of Phase II Data Collection

Field Site	Data Collection	Daily Outdoor Temperature (F)			HVAC Energy (kWh)	Energy Savings
		Maximum	Average	Minimum		
3 (Clear)	Baseline (1/5/10)	51	45	39	31.4	47%
	VCHP (1/24/16)	53	46	39	16.4	
4 (Ocala)	Baseline (1/13/10)	60	43	26	48.4	41%
	VCHP (1/24/16)	55	40	26	28.6	

Cooling Performance

Table 2-9 and Table 2-10 provide a cooling performance comparison for Field Sites 3 and 4 with the VCHP Phase II data and baseline heat pump data. For each site, a comparable period of weather was selected from baseline data for comparison. As discussed, ductwork modifications were performed at Field Site 3, and thus differences in the distribution system between the baseline and VCHP data collection may impact the energy consumption comparison. The rated equipment cooling efficiency at the sites from baseline to VCHP changed from 13.0 to 20.0 and 13.0 to 15.3 for Sites 3 and 4, respectively. For comparable outdoor conditions, the VCHP at Field Site 3 illustrated energy reductions of 26 – 28%, while the VCHP at Field Site 4 demonstrated energy reductions of 9 – 12%. The potential energy savings of VCHPs for cooling operation can be attributed to their increased designed cooling efficiency (e.g. increased SEER or EER), and their ability to operate at part-load with increased efficiency and reduced cycling.

Table 2-9
Site 3 – Cooling Comparison of VCHP to Baseline

Average Daily Outdoor Temp (F)	Daily HVAC Energy (kWh)		HVAC Peak Demand (kW)	
	Baseline	VCHP	Baseline	VCHP
75 - 80	16.7	12.4	2.5	2.1
80 - 85	24.7	17.8	2.7	2.0

Table 2-10
Site 4 – Cooling Comparison of VCHP to Baseline

Average Daily Outdoor Temp (F)	Daily HVAC Energy (kWh)		HVAC Peak Demand (kW)	
	Baseline	VCHP	Baseline	VCHP
75 - 80	19.1	17.4	3.0	2.6
80 - 85	28.3	24.7	3.4	2.3

Power Profile of VCHP Field Sites

Figure 2-7 provides the average power demand of all four VCHPs across both the heating and cooling season for Phase II data collection. The figure illustrates the average HVAC power demand (heat pump + backup electric heat) in 5°F outdoor temperature increments. Due to differences in weather, the upper and lower outdoor temperature limits may differ slightly for a given site and corresponding location. As seen in the figure for each VCHP implemented to eliminate backup electric heat (Sites 2, 3, and 4), the average winter peak demand is approximately equivalent to average summer peak demand for each site. This correlation occurs largely due to the absence or minimization of backup electric heat at Sites 2, 3, and 4. For most VCHPs, the nominal power demand is generally similar between cooling and heating operation for comparable loads. At Field Site 1 where the VCHP was not implemented to eliminate backup electric heat, the peak demand during the heating season is 6 – 7 kW greater than the peak demand for cooling operation. This increased peak demand for heating occurs due to the usage of backup electric heat; however, the VCHP at Field Site 1 demonstrated significant backup heat reduction and energy savings over the baseline system as described in the previous study [1].

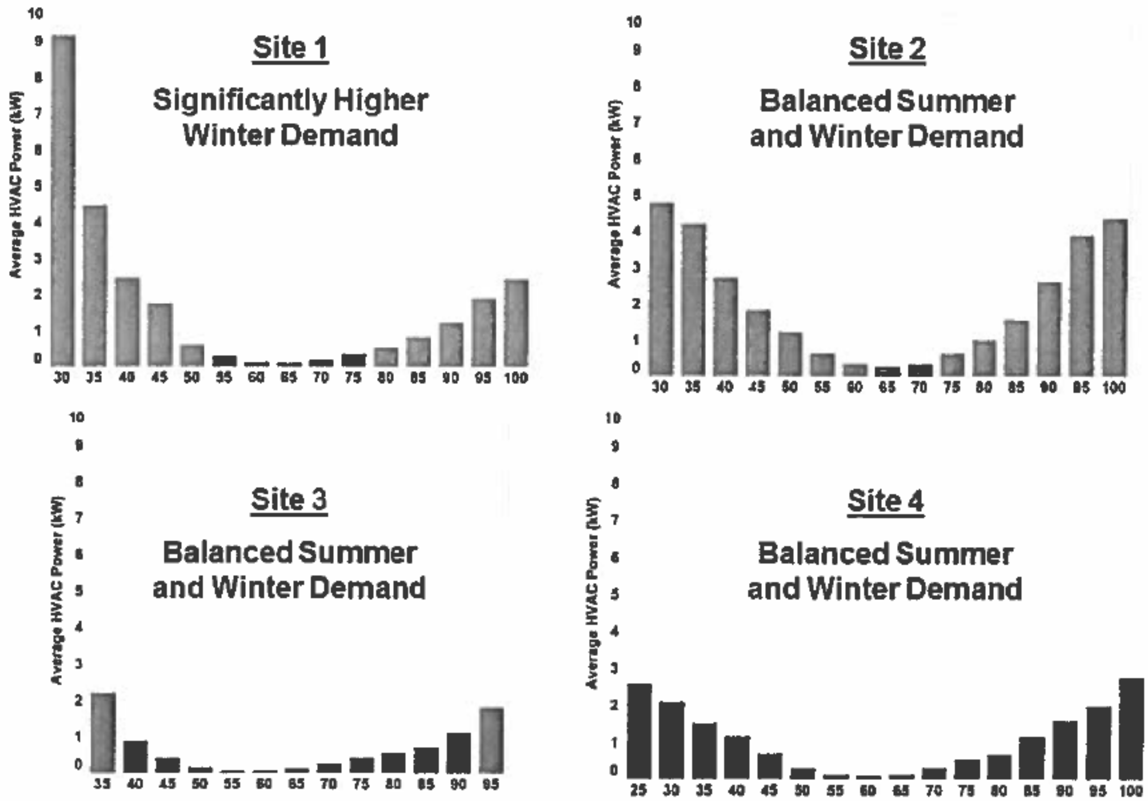

Figure 2-7
Annual Power Demand Profile of VCHP Field Sites for Phase II Data Collection

3
EFFECTIVENESS OF VCHPS

VCHP Equipment Cost

In the current residential HVAC market, VCHPs are considered a premium product with best-in-class efficiency and the incorporation of advanced features, such as high heating output at low temperatures and flexible demand response (DR) operation. As highlighted in Chapter 1, a range of VCHP products with unique characteristics are produced in the residential market. Table 3-1 provides a comparison in wholesale equipment cost between a 4-TON baseline heat pump and VCHP produced by a given manufacturer. The table breaks down the equipment cost by outdoor unit, indoor unit, controller, and backup electric heat. The baseline heat pump used for comparison was a 14 SEER, 8.2 HSPF unit, while the VCHP for comparison was an 18+SEER, 10.5+HSPF, high heating design system. The highest cost increase for a given component from the baseline to VCHP product is the outdoor unit, due to the incorporation of a variable speed compressor, variable speed condenser fan, and increased heat exchanger size.

Table 3-1
Wholesale Equipment Cost Comparison between 4-TON Baseline HP and VCHP

Heat Pump Component	Baseline Heat Pump (14 SEER, 8.2 HSPF)	VCHP (High Heating Design; 18+ SEER, 10.5+ HSPF)	Change in Cost
Outdoor Unit	$1,600 (1-Speed)	$3,300 (VS)	+$1,700
Indoor Unit	$850 (1-Speed)	$1,500 (VS)	+$650
Controller	$15 - $250 (Basic – Smart)	$400 (VS Compatible)	+$150
Backup Electric	$150	$100	-$50

Expanding on the wholesale equipment cost comparison in Table 3-1, Figure 3-1 compares the total wholesale equipment cost by nominal size (2 – 5 tons) for the same baseline and VCHP equipment. The wholesale cost increase from the examined baseline to VCHP is approximately $2,500 at all nominal size levels. From a retail cost perspective, baseline and VCHP equipment may be subject to an ~1.5 multiplier to account for product installation and the overall cost to the contractor. Fundamentally, the installation of a baseline heat pump and a VCHP is identical. A percentage of contractors, who are unfamiliar with VCHPs, may view VCHPs as complex with advanced installation requirements. These contractors may use a higher cost multiplier when quoting VCHPs to account for the perceived complexity or to avoid the installation of VCHPs.

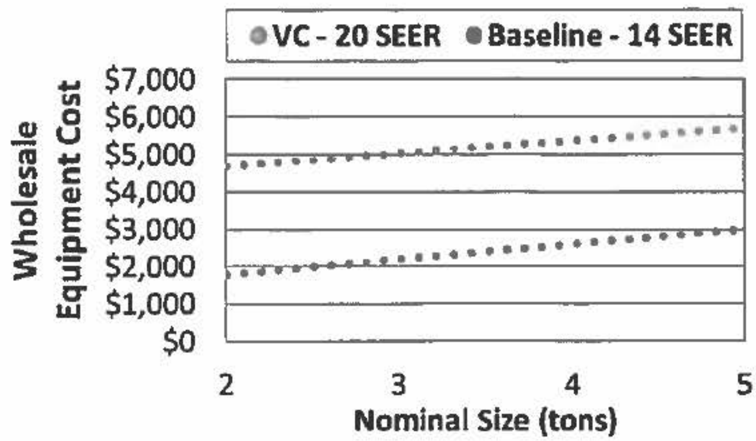

Figure 3-1
Wholesale Cost Comparison of Baseline HP and VCHP for Varying Nominal Size

Utility and Customer Effectiveness

In order to explore the utility and customer effectiveness of VCHPs for Central Florida, six unique cases were developed for consideration. The six VCHP cases are described in Table 3-2, Table 3-3, and Table 3-4. Each case illustrates a potential scenario for eliminating backup electric with VCHPs in Central Florida residences. Each of the three general categories considered in this research study for VCHP implementation was considered: a. oversized, high heating VCHP, b. high heating VCHP, and c. standard heating, cost competitive VCHP. Two levels of annual energy savings were assumed for each general category. The assumptions and data outlined in the six cases were developed based on project findings, field data analysis, energy modeling, and industry surveys. Table 3-2 provides the assumed VCHP equipment characteristics for each case including rated efficiency, heating design, and whether the system was oversized. Table 3-3 provides the assumed annual energy savings, cooling peak demand reduction, and heating peak demand reduction. Table 3-4 provides the assumed wholesale and retail cost increase from a baseline to VCHP.

Table 3-2
VCHP Product Characteristics for Utility and Customer Test Cases

Description	Case	SEER	HSPF	VCHP Product		
				High Heating Output Design	Oversized for Cooling	Cost Comp., Standard Heating
Oversized HH-VCHP	1 2	18+	10.5+	✓	✓	
HH-VCHP	3 4	18+	10.5+	✓		
Cost Comp. VCHP	5 6	18+	10+			✓

1. High Heating Output Design refers to VCHPs capable of providing ~100% nominal capacity at 17°F.
2. Standard Heating Design refers to VCHPS capable of providing ~80% of nominal capacity at 17°F.

Table 3-3
VCHP Performance for Utility and Customer Test Cases

Description	Case	Annual Energy Saved (kWh)	Peak Cooling Demand Reduction (kW)	Peak Heating Demand Reduction (kW)
Oversized HH-VCHP	1	2,000	0	5
	2	3,000		
HH-VCHP	3	2,000	0.5	5
	4	3,000		
Cost Comp. VCHP	5	2,000	0.5	2.5
	6	3,000		

Table 3-4
Estimated Wholesale and Retail Cost Increase of VCHP Product Categories

Description	Case	Wholesale Cost Increase	Retail Cost Increase
Oversized HH-VCHP	1	$3,250	$4,875
	2		
HH-VCHP	3	$2,500	$3,750
	4		
Cost Comp. VCHP	5	$2,000	$3,000
	6		

Utilizing the developed six cases for VCHP implementation, utility and customer effectiveness tests were conducted using standard utility assumptions. Table 3-5 and Table 3-6 provide the Total Resource Cost (TRC), Rate Impact Measure (RIM), and Participant test for each of the six cases for the wholesale and retail cost increase, respectively. From the TRC and participant test perspective, the implementation of VCHPs was generally most effective for applications with higher annual HVAC energy savings and for cases in which the VCHP sizing was similar to baseline. Annual HVAC energy savings would be based on selected VCHP equipment (e.g. 4-ton, 18 SEER) and thermal load characteristics (e.g. 2,000 ft^2 residence in Orlando climate). TRC ratios near or above 1.0 were observed for both cost competitive and high heating VCHPs which were sized similar to baseline. The implementation of VCHPs was generally least effective for applications with lower annual energy savings and for cases in which oversizing the VCHP was required to eliminate backup heat. The reduced effectiveness of oversized VCHPs is primarily due to the increased cost of stepping up to a higher nominal size for an already premium product.

Table 3-5
Utility and Customer Effectiveness Tests for Wholesale Cost Differential

Description	Case	Total Resource Cost (NPV) (B-C Ratio)	Rate Impact Measure (NPV) (B-C Ratio)	Participant (NPV) (B-C Ratio)
Oversized HH-VCHP	1	-$793 (0.76)	-$116 (0.96)	-$1,186 (0.64)
	2	$61 (1.02)	-$548 (0.86)	-$154 (0.95)
HH-VCHP	3	$538 (1.22)	$465 (1.18)	-$436 (0.83)
	4	$1,392 (1.56)	$33 (1.01)	$596 (1.24)
Cost Comp. VCHP	5	$664 (1.33)	$91 (1.04)	$64 (1.03)
	6	$1,518 (1.76)	-$341 (0.91)	$1,096 (1.55)

Table 3-6
Utility and Customer Effectiveness Tests for Retail Cost Differential

Description	Case	Total Resource Cost (NPV) (B-C Ratio)	Rate Impact Measure (NPV) (B-C Ratio)	Participant (NPV) (B-C Ratio)
Oversized HH-VCHP	1	-$2,418 (0.50)	-$116 (0.96)	-$2,811 (0.42)
	2	-$1,564 (0.68)	-$548 (0.86)	-$1,779 (0.64)
HH-VCHP	3	-$712 (0.81)	$465 (1.18)	-$1,686 (0.55)
	4	$142 (1.04)	$33 (1.01)	-$654 (0.83)
Cost Comp. VCHP	5	-$336 (0.89)	$91 (1.04)	-$936 (0.69)
	6	$518 (1.17)	-$341 (0.91)	$96 (1.03)

4
CONCLUSIONS

Key Project Findings

- Multiple, unique VCHPs have demonstrated an ability to eliminate backup electric heat in Central Florida residences. These unique VCHPs have included high heating output designs (~100% nominal heating at 17°F) and standard heating designs (~80% nominal heating at 17°F). To eliminate backup electric heat in Central Florida residences, high heating output VCHPs were generally necessary for colder territories (e.g. inland: Orlando and Ocala), while standard heating VCHPs (including cost competitive versions) were effective in milder territories (e.g. coastal: Clearwater).
- During Phase II data collection, each of the three sites that were specified to eliminate backup heat (oversized Orlando, Clearwater, and Ocala) demonstrated an ability to sufficiently heat the residence with little-to-no backup electric heat usage during the coldest outdoor conditions.
- From a TRC and participant perspective, the implementation of VCHPs was generally most effective for applications with higher annual HVAC energy savings and for cases in which the VCHP sizing was similar to baseline. Annual HVAC energy savings would be based on selected VCHP equipment (e.g. 4-ton, 18 SEER) and thermal load characteristics (e.g. 2,000 ft^2 residence in Orlando climate). TRC ratios near or above 1.0 were observed for both cost competitive and high heating VCHPs which were sized similar to baseline. The implementation of VCHPs was generally least effective for applications with lower annual energy savings and for cases in which oversizing the VCHP was required to eliminate backup heat. The reduced effectiveness of oversized VCHPs is primarily due to the increased cost of stepping up to a higher nominal size for an already premium product.

Potential Program Implementation

The following points aim to provide guidance toward the consideration of a utility program for the implementation of VCHPs to eliminate backup electric heat usage in Central Florida:

- The implementation of VCHPs to eliminate backup electric heat could be a foreign concept to most HVAC contractors and program implementers. Learning aids and opportunities informing appropriate stakeholders could be key for successful program implementation. HVAC contractors may view backup electric heat as a "safety net" for heat pump malfunctions or improper equipment sizing.
- In order to guarantee the elimination of backup electric heat in VCHPs, specific unit settings for "backup heating" should be adjusted appropriately. This may include an "outdoor temperature lockout" for backup heat. In this research effort, an outdoor temperature lockout for backup electric heat was utilized at Field Site 2 and 3. This lockout prevents backup heat activation due to an increase in indoor setpoint temperature, which has been shown to be a common response in available VCHPs. The outdoor temperature lockout could be set at the "peak" heating condition or balance point for the location and residence. Backup electric heat during defrost operation occurred every 40 to 45 minutes for a duration of 3 to 4 minutes at

Field Sites 2 and 3 during outdoor temperatures between 25°F to 40°F. In aggregate, sporadic backup electric heat during the defrost cycles of VCHPs should have a lesser impact on utility peak demand.

- In order to balance defrost operation and for emergency situations, backup electric heat may be necessary for certain VCHP installations. Utilizing a *smaller* backup electric heat element (e.g. 5 kW) could assist in the overall VCHP performance for efficiency and peak demand. This strategy was utilized at Field Site 2 in this research study.
- From a practical standpoint, *accurate* Manual J load calculations, VCHP manufacturer performance data, and AHRI rating data can be utilized to properly consider and implement a VCHP for backup heat elimination. These data sets were the primary source of information for the VCHP implementations at Field Sites 2, 3, and 4.
- Rated efficiency levels (e.g. SEER, EER, HSPF, or COP) which are most effective for program implementation should be utilized. VCHPs are available from approximately 15 to 20+ SEER and approximately 10 to 13 HSPF.

5
REFERENCES

1. *Elimination of Electric Strip Heat Dependence with Advanced Inverter Driven Heat Pumps.* EPRI, Palo Alto, CA: 2015. 3002004964.
2. Air-Conditioning, Heating, and Refrigeration Institute Directory of Product Performance. https://www.ahridirectory.org/Search/SearchHome?ReturnUrl=%2f
3. *Residential Load Calculation* Manual J. Air Conditioning Contractors of America (ACCA). Hank Rutkowski. November 2011.
4. Weather Underground https://www.wunderground.com.

Export Control Restrictions

Access to and use of EPRI Intellectual Property is granted with the specific understanding and requirement that responsibility for ensuring full compliance with all applicable U.S. and foreign export laws and regulations is being undertaken by you and your company. This includes an obligation to ensure that any individual receiving access hereunder who is not a U.S. citizen or permanent U.S. resident is permitted access under applicable U.S. and foreign export laws and regulations. In the event you are uncertain whether you or your company may lawfully obtain access to this EPRI Intellectual Property, you acknowledge that it is your obligation to consult with your company's legal counsel to determine whether this access is lawful. Although EPRI may make available on a case-by-case basis an informal assessment of the applicable U.S. export classification for specific EPRI Intellectual Property, you and your company acknowledge that this assessment is solely for informational purposes and not for reliance purposes. You and your company acknowledge that it is still the obligation of you and your company to make your own assessment of the applicable U.S. export classification and ensure compliance accordingly. You and your company understand and acknowledge your obligations to make a prompt report to EPRI and the appropriate authorities regarding any access to or use of EPRI Intellectual Property hereunder that may be in violation of applicable U.S. or foreign export laws or regulations.

The Electric Power Research Institute, Inc. (EPRI, www.epri.com) conducts research and development relating to the generation, delivery and use of electricity for the benefit of the public. An independent, nonprofit organization, EPRI brings together its scientists and engineers as well as experts from academia and industry to help address challenges in electricity, including reliability, efficiency, affordability, health, safety and the environment. EPRI members represent 90% of the electric utility revenue in the United States with international participation in 35 countries. EPRI's principal offices and laboratories are located in Palo Alto, Calif.; Charlotte, N.C.; Knoxville, Tenn.; and Lenox, Mass.

Together...Shaping the Future of Electricity

3002014920

Electric Power Research Institute
3420 Hillview Avenue, Palo Alto, California 94304-1338 • PO Box 10412, Palo Alto, California 94303-0813 • USA
800.313.3774 • 650.855.2121 • askepri@epri.com • www.epri.com

Attachment C

Sustainable Electric Energy Delivery Systems (SEEDS) 3

Project Report

Smart Grid Power Systems Lab

May, 2018

University of South Florida
Department of Electrical Engineering

Project Director
Mr. George Gurlaskie
Duke Energy Business Services
3300 Exchange Place, NP2A
Lake Mary, FL 32746
(407)942-9381
(407)942-9388
George.gurlaskie@pgmail.com

USF PI
Dr. Lingling Fan
4202 E. Fowler Ave., ENB 118
Dept. of Electrical Engineering
Tampa, FL 33620
(813)974-2031
(813)974-5525
linglingfan@usf.edu

USF Co-PI
Dr. Zhixin Miao
4202 E. Fowler Ave., ENB 118
Dept. of Electrical Engineering
Tampa, FL 33620
(813)974-4237
(813)974-5525
zmiao@usf.edu

Graduate Students:

Miao Zhang, Ph.D. student
miaozhang@mail.usf.edu

Yangkun Xu, Ph.D. student
yangkunxu@mail.usf.edu

Yi Zhou, Ph.D. student
yizhou@mail.usf.edu

Li Bao, Ph.D. student
libao@mail.usf.edu

Contents

Chapter 1

Introduction

Two photovoltaic-battery systems were installed at University of South Florida (USF) St. Petersburg campus (Battery 1) and at Albert Whitted Park at St. Petersburg downtown (Battery 2) to realize smart grid functionalities: peak shaving and/or demand response. Currently each PV is connected to the grid through an inverter, while the two batteries are 5kW-4 hours Li-ion batteries and equipped with a charger and an inverter. The rated dc voltage of each battery is 48 V. The ac side of the battery at the USF St. Petersburg campus is connected to a 120/208 V panel. The ac side of the battery at the Albert Whitted park is connected to a 120/240 V panel.

The configuration of the PV-battery system is shown in Fig. 1.1.

The two batteries are operated in two modes. The first one is operated for peak shaving and energy shift. The second one is operated to realize demand response.

(1) Peak shaving provided by a PV/battery system with constant output power
The PV/battery system is expected to provide constant output power at peak periods, Summer (14:00-20:00) and Winter (06:00-10:00). The net output of the SEEDS system (PV and battery) will be held at 1.6 kW. The battery will be charged to a minimum available energy of 10kWh prior to 6AM daily. The charging will commence at midnight and be done by 5 am daily. Off-peak energy and/or available solar PV energy will be used for the charging.

(2) Demand response by a PV/battery system with maximum output power
The second PV/battery system will also be charged during off-peak period. Full 5 kW discharge capacity of the charged battery system and PV output will be delivered to the system whenever there is a command.

Approach and requirements to realize smart grid functions Remote real-time control and monitoring system is required to develop the above mentioned smart grid functions. In order to realize the remote control and monitoring, the following requirements must be met:

(1) Measurements such as power, voltage, current flowing into or out from the ac side of the battery system should be obtained constantly. Energy can be computed based on these measurements.

(2) Measurements such as temperature, dc voltage, dc currents, battery SOC for a battery should be monitored.

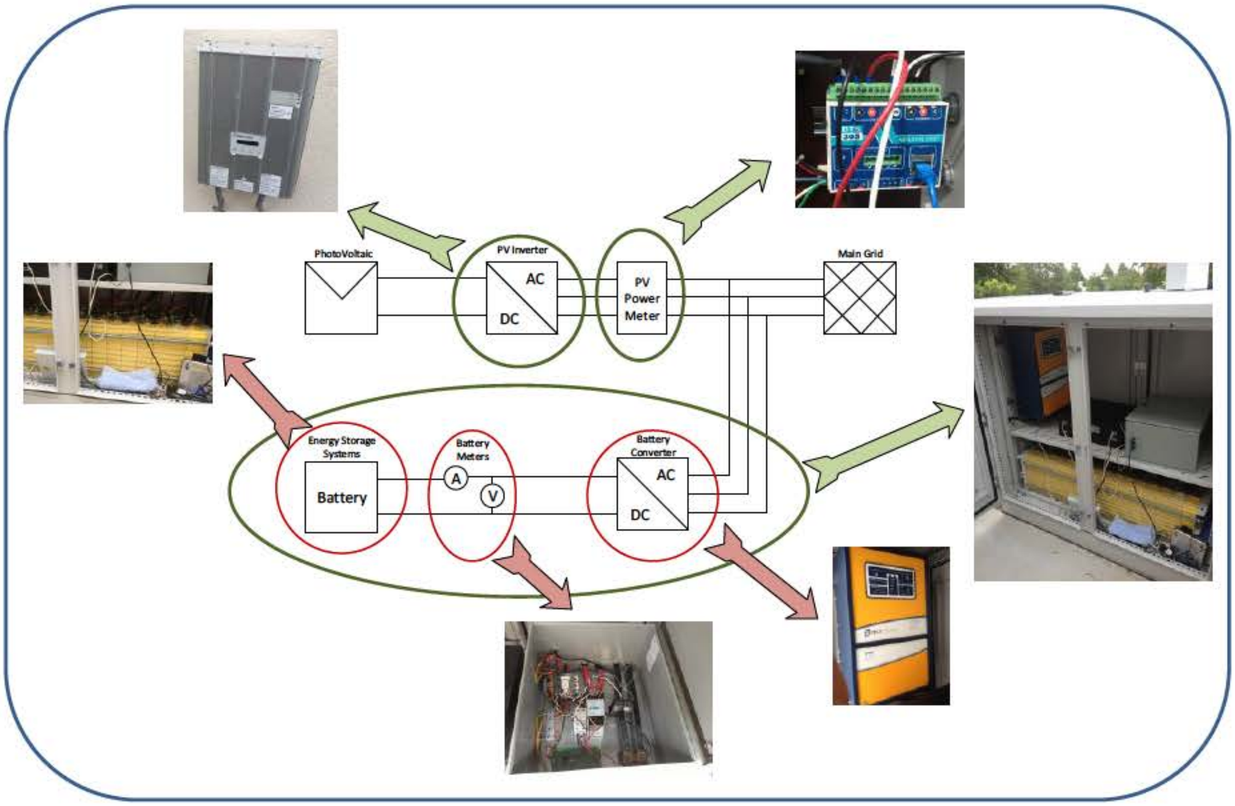

Figure 1.1: Configuration of Photovoltaic-Battery systems in both campus and airport sites.

(3) The human machine interfaces (HMI) provided by the battery vendor (Green Smith) should be able to execute inverter control to charge and discharge the battery system.

(4) Measurements from the PV output should be available for the operator to do calibration.

Our team's work. During the project period of SEEDS projects (2013- Dec. 2016), the USF SPS team reviews data and produces a weekly report with plots of two batteries's power and energy and conducts data analysis with accumulated data. The USF team also responds to abnormal conditions, diagnoses the root courses, and fixes the issues.

Total, the following trips were made to St. Petersburg from 2015 to 2017.
4/01/2015 USF Tampa to USF St. Pete
4/02/2015 USF Tampa to USF St. Pete
4/15/2015 USF Tampa to USF St. Pete
4/30/2015 USF Tampa to USF St. Pete
5/20/2015 USF Tampa to USF St. Pete
6/12/2015 USF Tampa to USF St. Pete
6/30/2015 USF Tampa to USF St. Pete
7/1/2016 USF Tampa to Albert Whitted Park
7/2/2016 USF Tampa to Dan Wheldon Way, St. Pete

7/8/2016 USF Tampa to Albert Whitted Park
1/13/2017 USF Tampa to Albert Whitted Park
2/20/2017 USF Tampa to USF St. Pete Campus

The major upgrades related to the PV and battery systems are as follows.

1. In the middle of 2015, the data communication service of the Campus side battery provided by Clear Communication was interrupted due to the purchase of Clear Communication by Sprint. Multiple trips were made to the site to first diagnose the cause of not receiving data at USF Tampa office, conduct tests, find the cause and finally switch the communication service to Verizon and conduct tests onsite for data communication.

2. In May 2016, measurements from the airport battery system became abnormal. Multiple trips were made to the sits to conduct tests to diagnose the cause. It was found the damage was due to a DC meter installed by EPRI, which was burned and in turn lead to the burn of the entire circuit related to the airport PV inverter. The PV inverter was damaged. Due to the discontinuity of the product, the PV inverter manufacturer spent time finding a matching inverter. The installation was finished in January 2017. Trips were made in January 2017 to help the installation by the inverter company as well as conducting tests to make data communication work.

3. In Feb 2017, over voltage was observed for the campus site battery. Trips were made and it was found that the over voltage was due to a cell of battery no longer functioning.

The overall summary is presented in Table 1.1.

Table 1.1: Summary Numbers

Average 2013-2016 Campus battery daily kWh:	6.37 kWh
Average 2013-2016 Airport battery daily kWh:	6.91 kWh
Number of days the campus Battery operates to discharge more than 1 kW:	883 days
Number of days the campus battery operates to discharge more than 0.1 kW:	905 days
Number of days the airport battery operates to discharge more than 3 kW:	170 days
Number of days the airport battery operates to discharge more than 1kW:	586 days

Chapter 2

Measurement Data and Related Data Handling

Two sets of measurements are obtained from the SEEDS project: (1) EPRI data; (2) Greensmith data. The raw data are stored in csv text files. Those files can be opened by Microsoft's Excel and shown as spreadsheets.

2.1 EPRI Data

Fig. 2.1 shows the raw data in csv files and Fig. 2.2 shows the details of an EPRI data file.

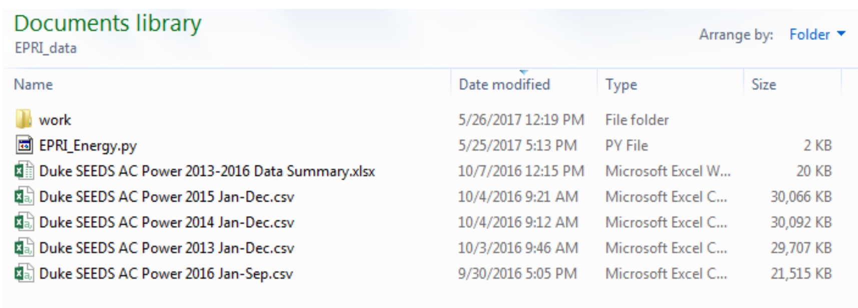

Figure 2.1: Raw data as csv files. Data resolution: 1 minute.

The EPRI data gives Time, and measurement from the four power meters installed at campus PV, campus battery, airport PV and airport battery. The number of records every year is listed in Table 2.1. Approximately 525,600 data points were collected for a whole year except data outages.

2.2 Greensmith Data

The Greensmith data include battery dc voltage, dc current and state of charge (SOC) besides ac power measurements from the battery and the PV. Table 2.2 provides the specification of the data collected for each battery.

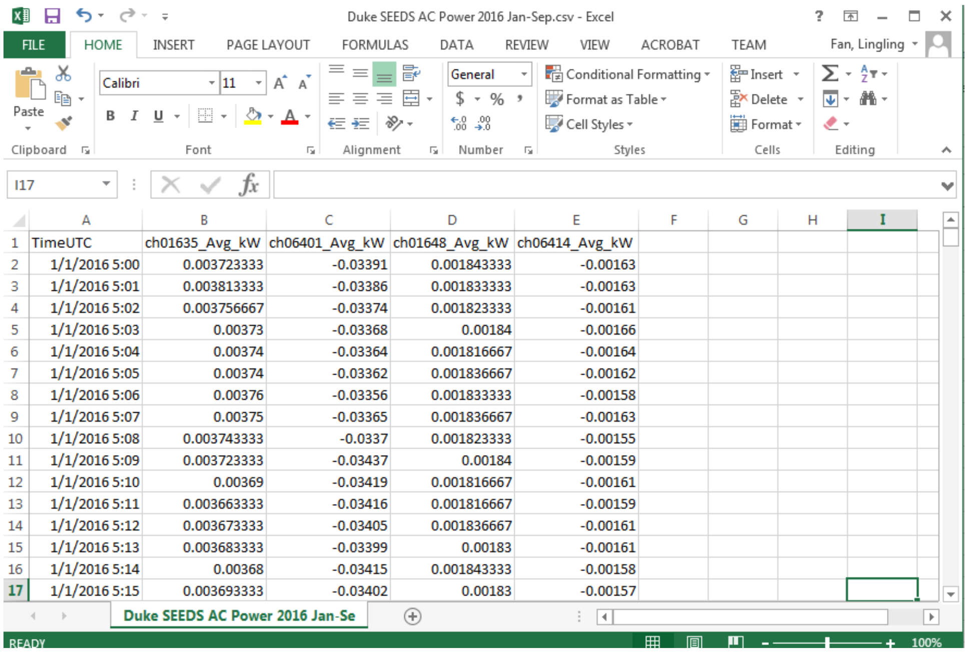

	TimeUTC	ch01635_Avg_kW	ch06401_Avg_kW	ch01648_Avg_kW	ch06414_Avg_kW
2	1/1/2016 5:00	0.003723333	-0.03391	0.001843333	-0.00163
3	1/1/2016 5:01	0.003813333	-0.03386	0.001833333	-0.00163
4	1/1/2016 5:02	0.003756667	-0.03374	0.001823333	-0.00161
5	1/1/2016 5:03	0.00373	-0.03368	0.00184	-0.00166
6	1/1/2016 5:04	0.00374	-0.03364	0.001816667	-0.00164
7	1/1/2016 5:05	0.00374	-0.03362	0.001836667	-0.00162
8	1/1/2016 5:06	0.00376	-0.03356	0.001833333	-0.00158
9	1/1/2016 5:07	0.00375	-0.03365	0.001836667	-0.00163
10	1/1/2016 5:08	0.003743333	-0.0337	0.001823333	-0.00155
11	1/1/2016 5:09	0.003723333	-0.03437	0.00184	-0.00159
12	1/1/2016 5:10	0.00369	-0.03419	0.001816667	-0.00161
13	1/1/2016 5:11	0.003663333	-0.03416	0.001816667	-0.00159
14	1/1/2016 5:12	0.003673333	-0.03405	0.001836667	-0.00161
15	1/1/2016 5:13	0.003683333	-0.03399	0.00183	-0.00161
16	1/1/2016 5:14	0.00368	-0.03415	0.001843333	-0.00158
17	1/1/2016 5:15	0.003693333	-0.03402	0.00183	-0.00157

Figure 2.2: Data stored in the EPRI data file. Data from four power meters are listed: campus PV, campus battery, airport PV, and airport battery.

Table 2.1: EPRI Data Summary

year	# of records	Missed data	Percentage	Data Outage Comments
2013	525,600	48.501	97.69%	- all energy storage channels (channels 6401, 6414) 2013-01-01 05:00 to 2013-01-17 16:00 UTC - all USF Physical Plant channels (channels 1635, 6401: 2013-05-17 22:10 to 2013-05-17 22:44 UTC 2013-10-23 14:18 to 2013-10-23 16:42 UTC - all Albert Whitted Park channels (channels 1648, 6414): 2013-05-16 06:55 to 2013-05-16 18:45 UTC - all channels: 2013-05-16 12:30 to 2013-05-16 18:43 UTC 2013-06-02 00:11 to 2013-06-02 20:22 UTC
2014	525,600	422	99.98%	- all USF Physical Plant channels (channels 1635, 6401): 2014-11-20 13:07 to 2014-11-20 13:17 UTC - ll Albert Whitted Park channels (channels 1648, 6414): 2014-11-19 21:06 to 2014-11-19 21:12 UTC 2014-12-17 16:13 to 2014-12-17 17:21 UTC
2015	525,600	196	99.99%	- all Albert Whitted Park channels (channels 1648, 6414): 2015-04-24 15:06 to 2015-04-24 15:39 UTC 2015-05-23 14:31 to 2015-05-23 14:58 UTC
2016	393,060	262	99.98%	- all USF Campus (channels 1635, 6401): 2016-04-16 19:34 to 2016-04-16 20:31 UTC - all Albert Whitted Park (channels 1648, 6414): 2016-06-19 14:01 to 2016-06-19 15:16 UTC

Table 2.2: Greensmith data specification

Column #	Measurement
1	Id
2	Recorded Time
3	State of Charge
4	State Of Health
5	Cell Volt(min)
6	Cell Volt Location(min)
7	Cell Volt(max)
8	Cell Volt Location(max)
9	Cell Temperature(min)
10	Cell Temperature Location(min)
11	Cell Temperature(max)
12	Cell Temperature Location(max)
13	AC Real Power(W)
14	AC Reactive Power(W)
15	DC Current
16	DC Volt
17	Energy Chargeable(Wh)
18	Energy Dischargeable(Wh)
19	Load Power
20	Meter Power: PV_Meter(W)
21	Meter Var: PV_Meter(W)

An example csv file related to the 2016 Airport data is shown in Fig. 2.3. The number of data points collected every year is shown in Table 2.3. Compared to the EPRI measurements, Greensmith system collects less data points due to data communication network unavailability. Since Greensmith system collects more measurements compared to the EPRI measurement system, Greensmith system also suffers less reliability in data communication.

Table 2.3: GreenSmith Data Summary

Year	Location	Data Points	Comments
2013	Campus	474,597	
2013	Airport	444,848	
2014	Campus	480,883	
2014	Airport	442,975	
2015	Campus	406,851	Data communication outages
2015	Airport	380,885	Data communication outages
2016	Campus	392,713	
2016	Airport	226,714	Inverter damage causes less data points

	A	B	C	D	E	F	G	H	I	J	K	L	M	N	O	P	Q	R	S	T	U	V
1	Id	Recorded Time	State of C	State Of H	Cell Volt(	Cell Volt L	Cell Volt(	Cell Volt L	Cell Temp	Cell Temp	Cell Temp	Cell Temp	AC Real P	AC Reacti	DC Curren	DC Volt	Energy Ch	Energy Di	Load Pow	Meter	Meter Var: PV_Meter(W)	
2	16463732	1/1/2016 0:01	1.550297	100	3.059	T01C04	3.216	T01C03	28.8	T01C01	33.2	T01C05	-2	0	0	51.11	19965.6	298.6803	2	17	null	
3	16463738	1/1/2016 0:02	1.550297	100	3.059	T01C04	3.216	T01C03	28.8	T01C01	33.2	T01C05	-2	0	0	51.09	19965.6	298.6803	0	17	null	
4	16463744	1/1/2016 0:03	1.550297	100	3.059	T01C04	3.211	T01C03	28.8	T01C01	33.2	T01C05	-2	0	0	51.11	19965.6	298.6803	0	17	null	
5	16463750	1/1/2016 0:04	1.550297	100	3.059	T01C04	3.216	T01C03	28.8	T01C01	33.2	T01C05	-2	0	0	51.09	19965.6	298.6803	0	17	null	
6	16463756	1/1/2016 0:06	1.550297	100	3.059	T01C04	3.216	T01C03	28.8	T01C01	33.2	T01C05	-2	0	0	51.11	19965.6	298.6803	0	17	null	
7	16463762	1/1/2016 0:07	1.550297	100	3.059	T01C04	3.216	T01C03	28.8	T01C01	33.2	T01C05	-2	0	0	51.11	19965.6	298.6803	2	16	null	
8	16463768	1/1/2016 0:08	1.550297	100	3.059	T01C04	3.216	T01C03	28.8	T01C01	33.2	T01C05	-2	0	0	51.09	19965.6	298.6803	0	17	null	
9	16463774	1/1/2016 0:09	1.550297	100	3.059	T01C04	3.211	T01C03	28.8	T01C01	33.2	T01C05	-2	0	0	51.13	19965.6	298.6803	0	17	null	
10	16463780	1/1/2016 0:11	1.550297	100	3.059	T01C04	3.216	T01C03	28.8	T01C01	33.2	T01C05	-2	0	0	51.09	19965.6	298.6803	0	17	null	
11	16463786	1/1/2016 0:12	1.550297	100	3.059	T01C04	3.211	T01C03	28.8	T01C01	33.2	T01C05	-2	0	0	51.09	19965.6	298.6803	0	17	null	
12	16463792	1/1/2016 0:13	1.550297	100	3.059	T01C04	3.216	T01C03	28.8	T01C01	33.2	T01C05	-2	2	0	51.09	19965.6	298.6803	0	17	null	
13	16463798	1/1/2016 0:15	1.550297	100	3.059	T01C04	3.216	T01C03	28.8	T01C01	33.2	T01C05	-2	0	0	51.11	19965.6	298.6803	0	16	null	
14	16463804	1/1/2016 0:16	1.550297	100	3.059	T01C04	3.216	T01C03	28.8	T01C01	33.2	T01C05	-2	0	0	51.09	19965.6	298.6803	0	17	null	
15	16463810	1/1/2016 0:18	1.550297	100	3.059	T01C04	3.216	T01C03	28.8	T01C01	33.2	T01C05	-2	2	0	51.09	19965.6	298.6803	0	17	null	
16	16463816	1/1/2016 0:19	1.550297	100	3.059	T01C04	3.216	T01C03	28.8	T01C01	32.7	T01C05	-2	2	0	51.11	19965.6	298.6803	0	16	null	
17	16463822	1/1/2016 0:20	1.550297	100	3.059	T01C04	3.211	T01C03	28.8	T01C01	33.2	T01C05	-2	0	0	51.09	19965.6	298.6803	2	17	null	
18	16463828	1/1/2016 0:21	1.550297	100	3.064	T01C04	3.216	T01C03	28.8	T01C01	32.7	T01C05	-2	0	0	51.09	19965.6	298.6803	2	16	null	
19	16463834	1/1/2016 0:22	1.550297	100	3.064	T01C04	3.216	T01C03	28.8	T01C01	32.7	T01C05	-2	0	0	51.09	19965.6	298.6803	0	17	null	
20	16463840	1/1/2016 0:25	1.550297	100	3.064	T01C04	3.216	T01C03	28.8	T01C01	32.7	T01C05	-2	0	0	51.09	19965.6	298.6803	0	17	null	
21	16463846	1/1/2016 0:26	1.550297	100	3.064	T01C04	3.216	T01C03	28.8	T01C01	32.7	T01C05	-2	0	0	51.09	19965.6	298.6803	0	17	null	
22	16463852	1/1/2016 0:27	1.550297	100	3.064	T01C04	3.216	T01C03	28.8	T01C01	32.7	T01C05	-2	0	0	51.09	19965.6	298.6803	0	17	null	
23	16463858	1/1/2016 0:28	1.550297	100	3.064	T01C04	3.216	T01C03	28.8	T01C01	32.7	T01C05	-2	0	0	51.13	19965.6	298.6803	2	18	null	
24	16463864	1/1/2016 0:30	1.550297	100	3.064	T01C04	3.216	T01C03	28.8	T01C01	32.7	T01C05	-2	0	0	51.13	19965.6	298.6803	0	17	null	
25	16463870	1/1/2016 0:31	1.550297	100	3.064	T01C04	3.216	T01C03	28.8	T01C01	32.7	T01C05	-2	2	0	51.09	19965.6	298.6803	0	18	null	

2016_Airport_DeviceStatus

Figure 2.3: Data stored in the Greensmith data file. Both dc side and ac side measurements are given.

2.3 Data Handling Tools

Due to the large size of the data file, directly using Excel to make plots takes a large amount of time. In addition, automatic plotting is difficult to be realized. In our data analysis work, we have conducted three tasks to make data analysis and plotting efficient.

- We have developed an SQL database to store four years' data in the database. Using query, we can then access the data fitting the query criteria. For example, we can list one week's data just by defining the time should be within a limit.
- Further, we have developed Python codes to access the database and make plots using Python module sqlite3.
- Alternatively, we used Python module pandas to directly access csv files and make plots.

The above tasks make data analysis efficient and possible.

SQL database

A database can be made using DB Browser SQLite. Fig. 2.4 shows the screen copy of the software. Click "File" and "import", the software gives choices to import data either from a database or from a table in a data file. Once the importing is complete, right click the table and modify the fields in the table as shown in Fig. 2.5. For example, TimeUTC type should be integer while the rest of the fields should have data type as numeric. With the database ready, we developed Python codes to access the database and conduct data analysis.

Python codes using sqlite3 to access database

Below is the Python code that access the database file (Duke SEEDS.db), select the data from January 22 to January 31 in 2013, and make plots. This code will plot one channel of the data.

The data query implemented in this code is

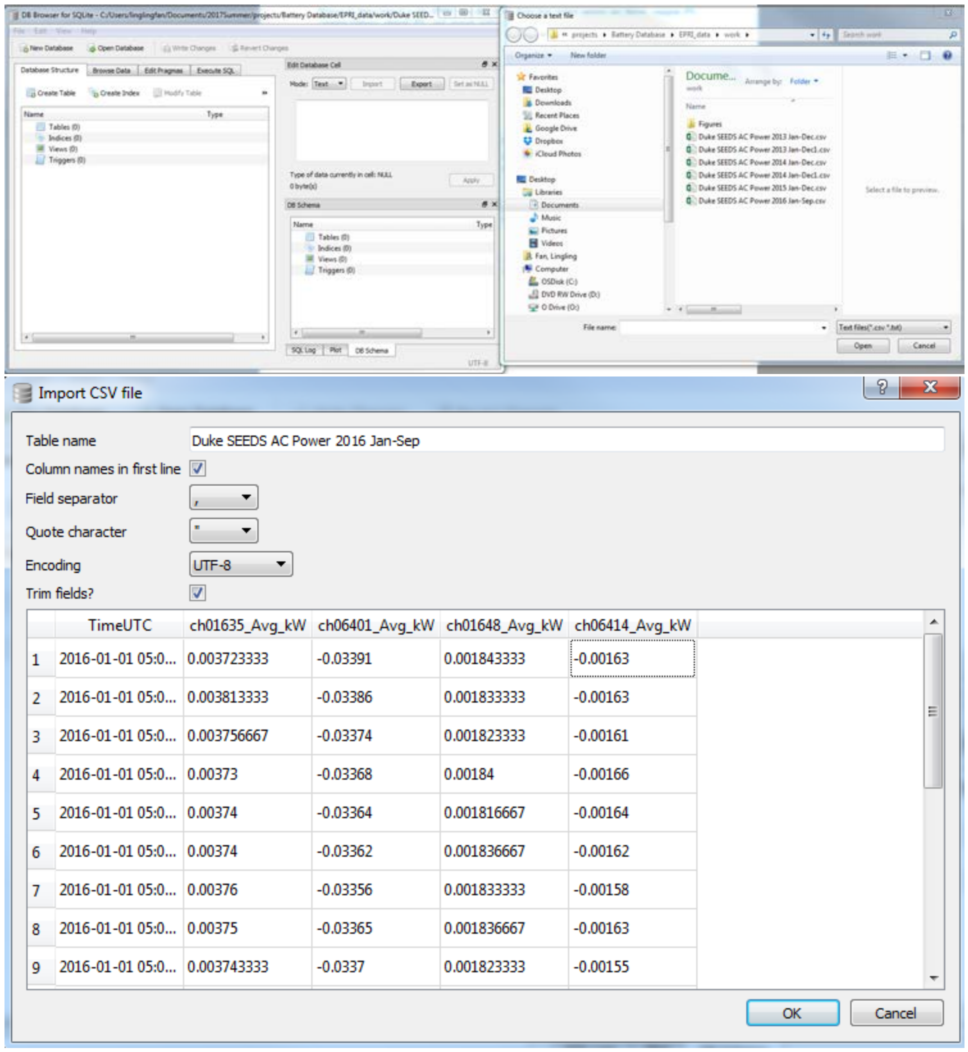

Figure 2.4: Importing csv files into a database. Step 1 and Step 2

```
SELECT TimeUTC, ch01648_Avg_kW\
                FROM "Duke SEEDS AC Power 2013 Jan-Dec"\
                WHERE date(TimeUTC)<("2013-02-01") AND date(TimeUTC)>("2013-01-21")’)
```

Changing the channel name “ch1648_Avg_kW”, we can access other columns of data. Changing the beginning and end data, we will access data of other periods.

Python codes:

```
import sqlite3
import time
import datetime
import random
import pylab
```

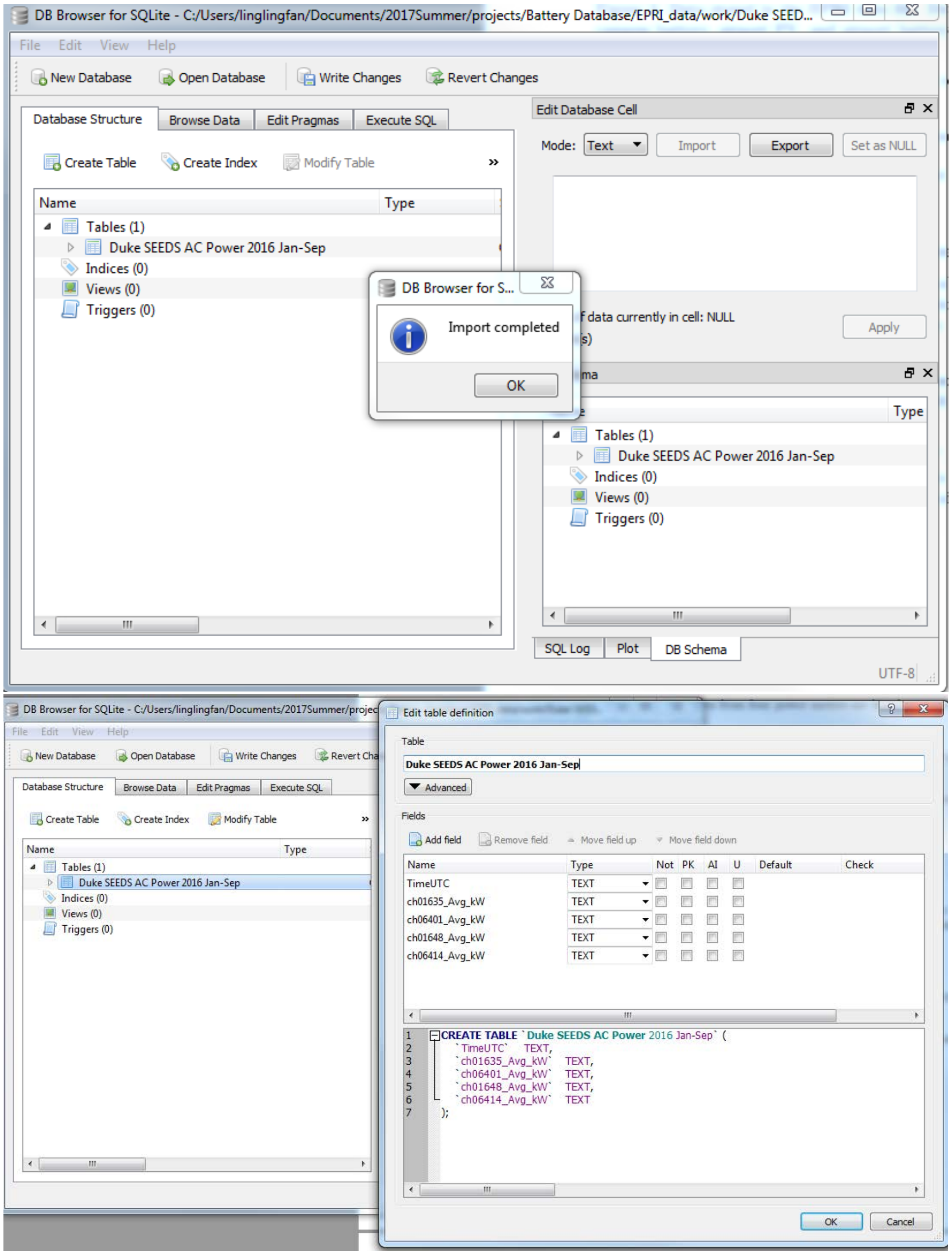

Figure 2.5: Importing csv files into a database. Step 3 and 4.

```
import matplotlib.pyplot as plt
import matplotlib.dates as mdates
from dateutil import parser
from matplotlib import style
style.use('fivethirtyeight')
```

```
conn = sqlite3.connect('Duke SEEDS.db')
c = conn.cursor()

def graph_data():
    c.execute('SELECT TimeUTC, ch01648_Avg_kW\
                FROM "Duke SEEDS AC Power 2013 Jan-Dec"\
                WHERE date(TimeUTC)<("2013-02-01") AND date(TimeUTC)>("2013-01-21")')
    data = c.fetchall()

    dates = []
    values = []

    for row in data:
        dates.append(parser.parse(row[0]))
        values.append(row[1])

    plt.plot_date(dates,values,'-')
    plt.title('ch01648_Avg_Power')
    plt.show()
    pylab.figure()
    pylab.plot(dates, values)
    pylab.savefig('/fig1.eps')
    pylab.close()

graph_data()
c.close
conn.close()
```

Python codes using pandas to access csv files

Alternatively, we also developed Python codes using module pandas to directly access the csv files. Below is an example code.

```
import pandas as pd
import datetime
import matplotlib.pyplot as plt
from matplotlib import style
import pytz

style.use('fivethirtyeight')

dfEPRI2013 = pd.read_csv('Duke SEEDS AC Power 2013 Jan-Dec.csv', usecols=[0, 4])
dfEPRI2014 = pd.read_csv('Duke SEEDS AC Power 2014 Jan-Dec.csv', usecols=[0, 4])
dfEPRI2015 = pd.read_csv('Duke SEEDS AC Power 2015 Jan-Dec.csv', usecols=[0, 4])
dfEPRI2016 = pd.read_csv('Duke SEEDS AC Power 2016 Jan-Sep.csv', usecols=[0, 4])
```

```
df = pd.concat([dfEPRI2013, dfEPRI2014, dfEPRI2015, dfEPRI2016])

df['Time'] = pd.to_datetime(df['TimeUTC']) - pd.DateOffset(hours=5)

df.set_index(df['Time'],inplace=True)
df = df.drop('TimeUTC', axis=1)
df = df.drop('Time', axis=1)


##df.index = df.index.tz_localize('UTC').tz_convert('US/Eastern')

##df.dropna(inplace=True)
##df['DC Power(W)'] = df['DC Current']*df['DC Volt']

df.dropna(inplace=True)

##df['ch06401_Charge_kWh'] = df['ch06401_Avg_kW_Pos']/60
##df['ch06401_Discharge_kWh'] = df['ch06401_Avg_kW_Neg']/60
df['Energy(kWh)'] = df.ch06414_Avg_kW.cumsum()/60
##df['Energy Dischargeable(Wh)'] = df['Energy Dischargeable(Wh)'].resample('D').mean()

#Fill NA by afterword method.

##df.fillna(method='pad',inplace=True)

##df['Diff'] = df['Daily_Charge_kWh'] + df['Daily_Discharge_kWh']

print(df)

fig = plt.figure()
ax1 = plt.subplot(2,1,1)
ax2 = plt.subplot(2,1,2, sharex=ax1)
##ax3 = plt.subplot(3,1,3, sharex=ax1)
##ax1.set_ylim([50, 100])
##ax2.set_ylim([19000, 20000])

df['ch06414_Avg_kW'].plot(color='r', ax=ax1).legend(shadow=True)
df['Energy(kWh)'].plot(color='b', ax=ax2).legend(shadow=True)
##df['DC Power(W)'].plot(color='m', ax=ax3).legend(shadow=True)
plt.suptitle('Power & Energy')
plt.show()
```

Chapter 3

Data Analysis

3.1 Data Availability

One-minute interval data are collected. The measurements come from the four power meters installed at campus PV, campus battery, airport PV and airport battery. Approximately 525,600 data points were collected for a whole year except data outages, which is shown in Fig. 3.1. Aside from ac power measurements, battery dc voltage, dc current and state of charge (SOC) are collected. The data are stored in spreadsheets as comma-separated values (csv)-based files.

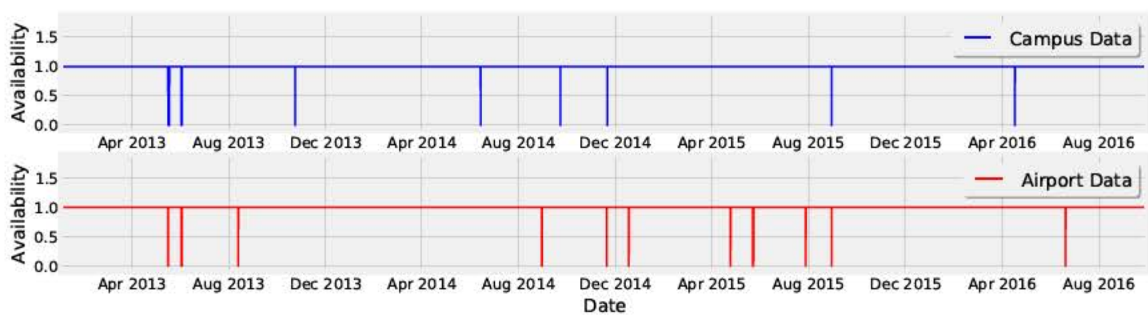

Figure 3.1: 2013-2016 Campus and Airport Data Availability.

Tables 3.1- 3.2 list the data outage starting time, end time and duration.

With the accumulated data, we have conducted statistics analysis, degradation analysis and system identification.

3.2 Data Analysis Results

3.2.1 PV/Battery Operation

Fig. 3.2 presents the ac power data in June 2013. Note the operation of campus battery and airport battery is to provide constant output power at 1:00 pm-7:00 pm. During each weekday morning, both batteries get charged using the PV power before 1:00 pm. Additionally, the campus battery gets charged in the early morning by the power from the utility grid to ensure enough energy for discharging operation in peak hours. Both those two batteries collaborate with PVs to

Table 3.1: Campus data outage records

Times	Start	End	Duration (min)
1	4/16/2016 19:34	4/16/2016 20:31	58
2	8/29/2015 20:20	8/29/2015 20:20	1
3	6/14/2014 1:10	6/14/2014 2:38	89
4	9/22/2014 9:14	9/22/2014 9:26	13
5	11/20/2014 13:07	11/20/2014 13:17	11
6	5/16/2013 12:30	5/16/2013 18:43	374
7	5/17/2013 22:10	5/17/2013 22:44	35
8	5/18/2013 3:43	5/18/2013 4:10	28
9	6/2/2013 0:11	6/2/2013 20:20	1210
10	10/23/2013 14:18	10/23/2013 16:42	145

Table 3.2: Airport data outage records

Times	Start	End	Duration (min)
1	6/19/2016 14:01	6/19/2016 15:16	73
2	4/24/2015 15:06	4/24/2015 15:39	34
3	5/22/2015 10:13	5/22/2015 10:34	22
4	5/23/2015 14:31	5/23/2015 14:58	28
5	7/28/2015 10:04	7/28/2015 10:15	12
6	8/29/2015 20:20	8/29/2015 20:20	1
7	8/30/2014 5:45	8/30/2014 6:06	22
8	11/19/2014 21:06	11/19/2014 21:12	7
9	12/17/2014 16:13	12/17/2014 17:21	69
10	5/16/2013 6:55	5/16/2013 18:45	711
11	6/2/2013 0:13	6/2/2013 20:22	1210
12	8/12/2013 23:56	8/12/2013 23:59	4
13	8/13/2013 0:00	8/13/2013 0:26	27

provide constant power in the afternoon. There is no discharging scheduled for those two batteries on weekend.

For the airport battery, 4 kW is discharged on June 24 and June 28. For the rest of the days in the week of June 24-July 1, the battery gets charged.

Fig. 3.3 gives the campus site PV/Battery system outputs in summer and winter operation strategies. The total power (in red color) indicates that the combined system can effectively shift to provide constant power during peak hours in Summer (14:00-20:00) and Winter (06:00-10:00). The PV/Battery device would keep zero output if there was no need.

The airport PV/Battery system's power plots are shown in Fig. 3.4 for the selected January, May and July 2013 data. From those plots, it can be seen that the airport battery gets charged till full and sends out power at 4 kW for a time block (4 hours) in January, May, and July.

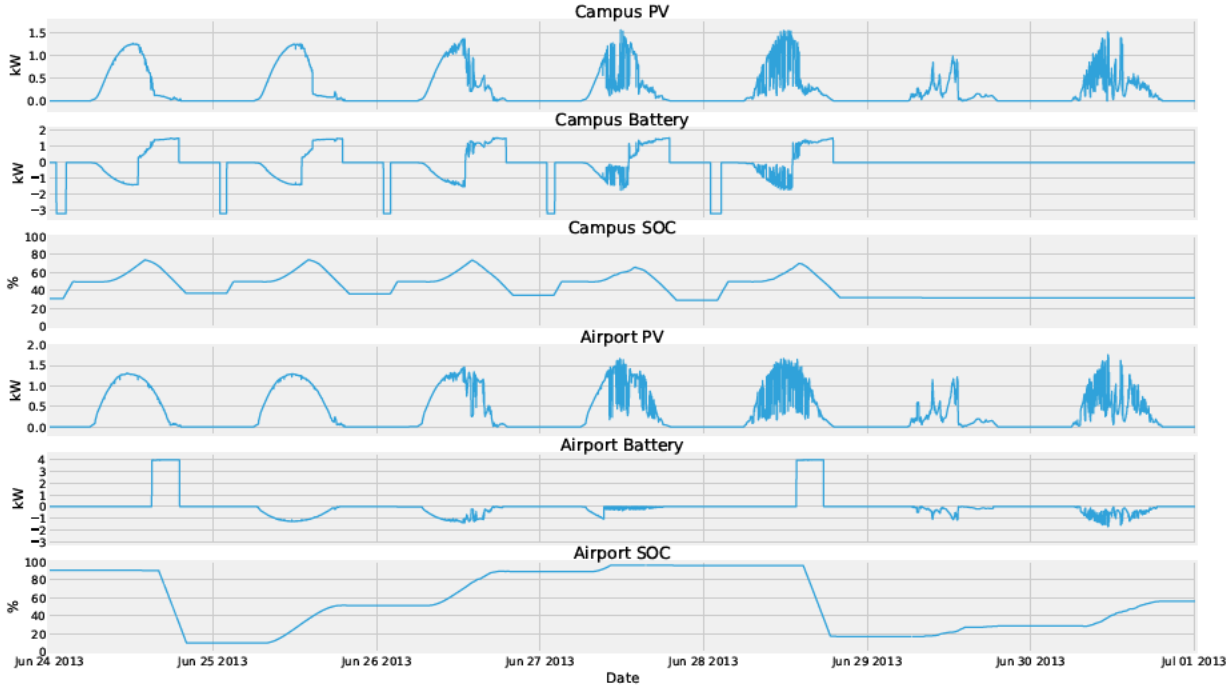

Figure 3.2: A week's data in June 2013. From top to bottom: campus PV, campus battery, campus battery SOC, airport PV, and airport battery, airport battery SOC. Note for batteries, reference power direction is assumed to be discharging.

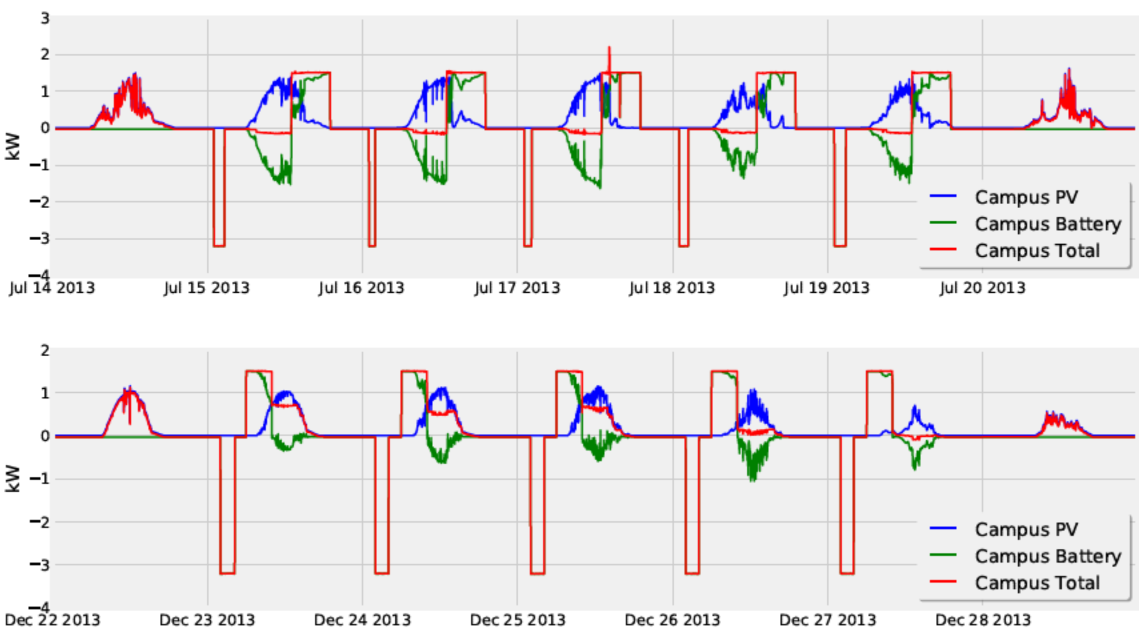

Figure 3.3: Campus PV/Battery system summer (upper one) and winter (lower one) operations.

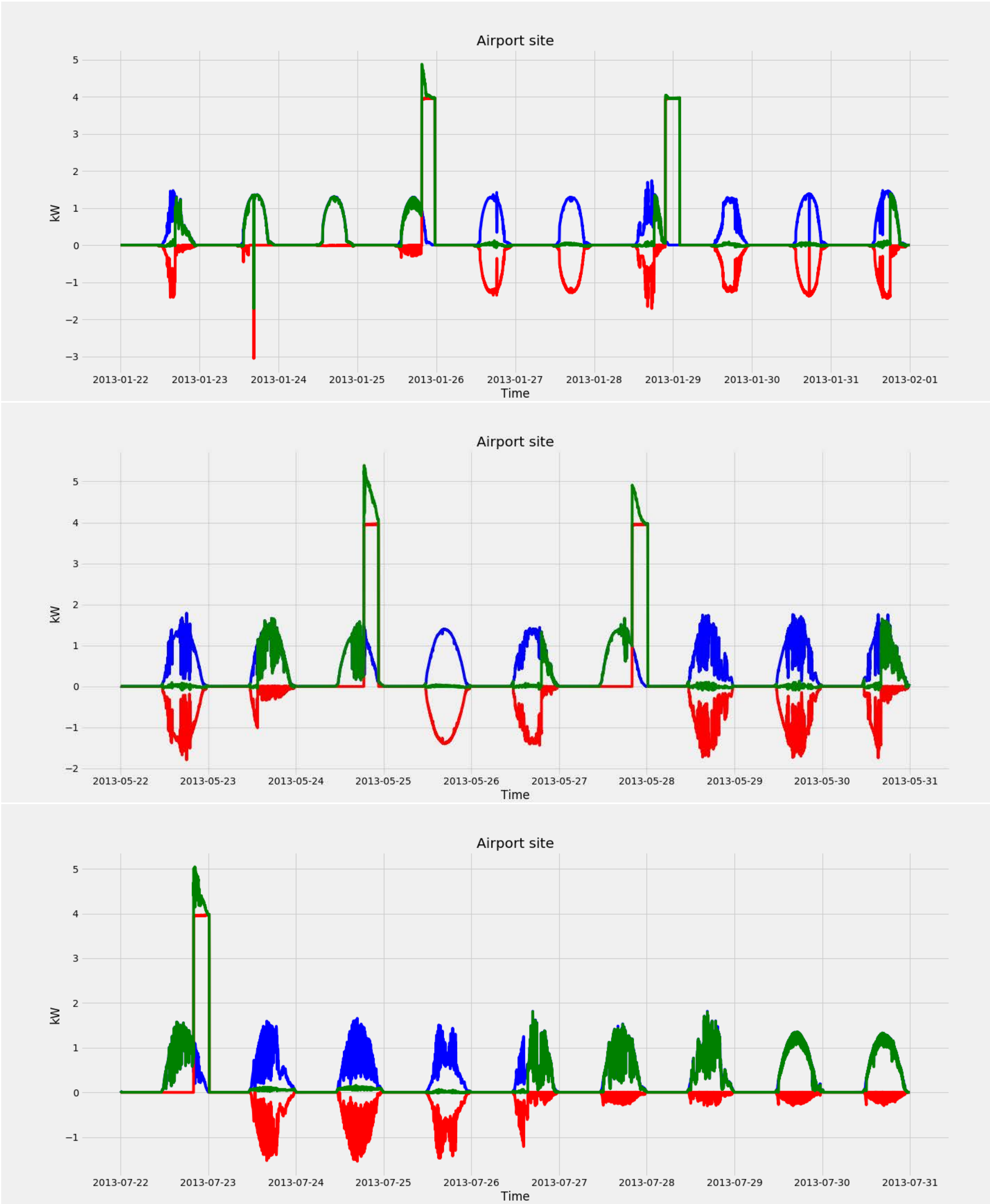

Figure 3.4: 2013 January, May and July Airport PV/batery system power output. Blue: PV; Red: Battery; Green: total.

3.2.2 PV Daily Energy

Fig. 3.5 and Fig. 3.6 present the four-year PV daily energy for the campus PV and airport PV, respectively. The campus PV daily energy capture capability was improved after 2014. This is due to the removal of a tree at the site. Shades of the tree prevented the solar PV to absorb radiation.

The airport PV daily energy plot can be used to examine the weather impact on PV output. It can be clearly seen that in Tampa area, solar power is abundant in April and May. Storms happen in August and September days. Hurrican Irma formed on August 30 2017, and dissipated on September 13 2017.

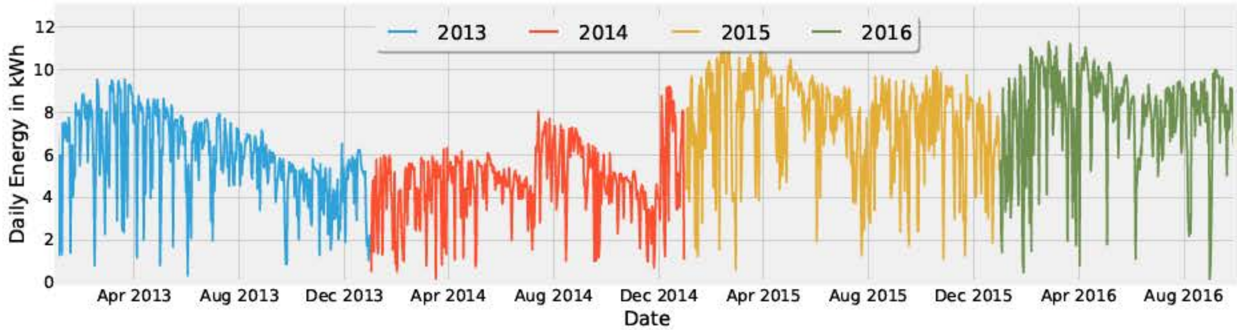

Figure 3.5: 2013-2016 campus PV daily energy in kWh.

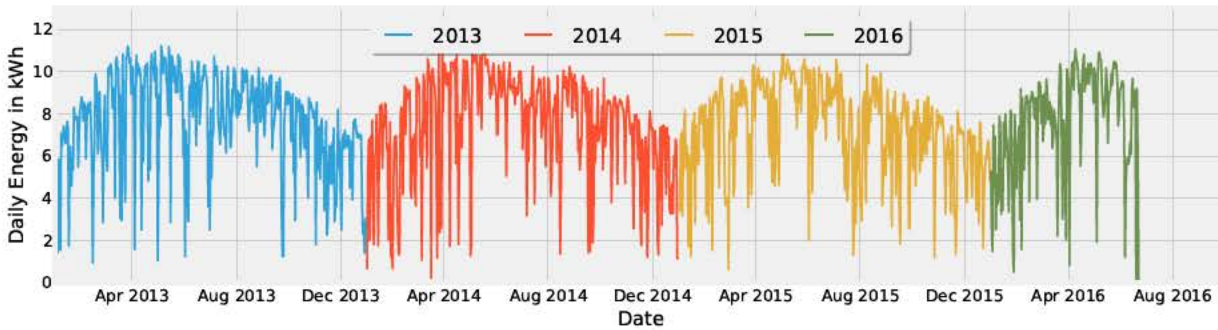

Figure 3.6: 2013-2016 airport PV daily energy in kWh.

The PV daily energy is computed from PV real-world power record. The record time interval is 1 minute. We approximately assumed the power was constant during each minute. Thus, we can sum up the power for a whole day to carry out the daily total PV energy through Python Pandas.

Few lines of Python code are given as follows. First, we calculate the PV energy per minute in kWh. Then the PV daily energy in kWh can be got by sum up one day's total data through `resample` function. Here, `df.airport_PV` is the original PV real-world data in per minute.

```
# Airport PV daily kWh
df['airport_PV_kWh'] = df.airport_PV/60
df_airport_PV_kWh_perday = \
df.airport_PV_kWh.resample('D', how='sum')
```

Therefore, each data in Fig. 3.5 and Fig. 3.6 is corresponding to the PV totally generated energy in one day.

```
>>> df_airport_PV_kWh_perday
TimeUTC
2013-01-01    7.449505
2013-01-02    6.687704
2013-01-03    2.467143
2013-01-04    1.435361
2013-01-05    5.839805
...
```

The histograms in Fig. 3.7 can be easily plotted using Python's Matplotlib module.

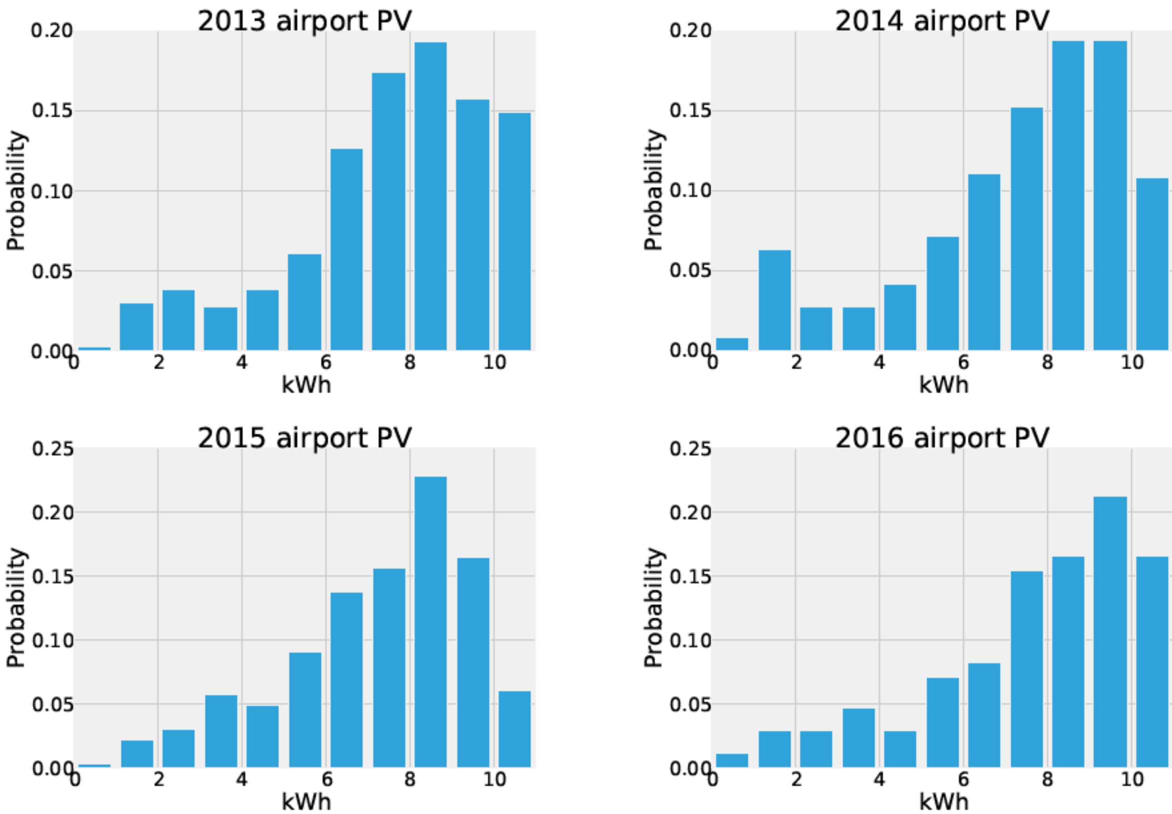

Figure 3.7: 2013-2016 airport PV daily energy histograms.

3.2.3 Battery Degradation Analysis

The battery degradation can be tested from two aspects. One is to check round-trip efficiency. Another is to check the battery chargeable capacity over time.

We use annual efficiency and sample efficiency to check battery round-trip efficiency. First, each year's annual efficiency is calculated through the battery output power spanning a whole year. We can treat one year as a long-term round-trip since the beginning SOC is closed to ending SOC for each year. The percentage of data outage is less than 1% so that we can ignore them. The ratio of the whole year's discharged energy to charged energy is the annual efficiency, shown in Fig. 3.8a. Overall, we see a decrease in round-trip efficiency.

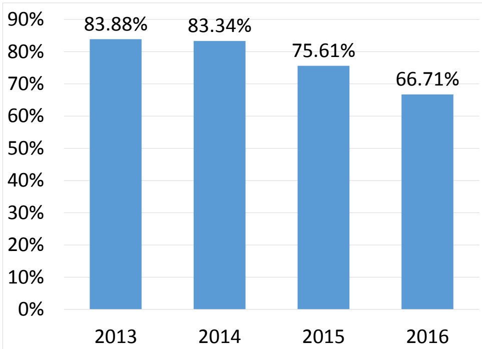

(a) Airport battery annual efficiency

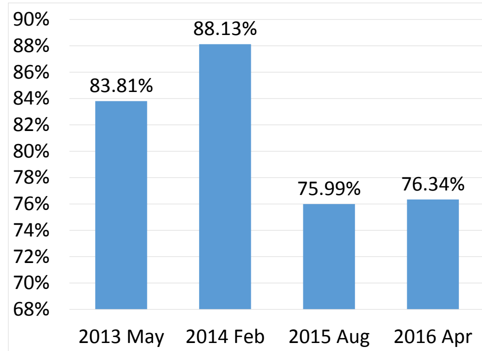

(b) Airport battery sample efficiency

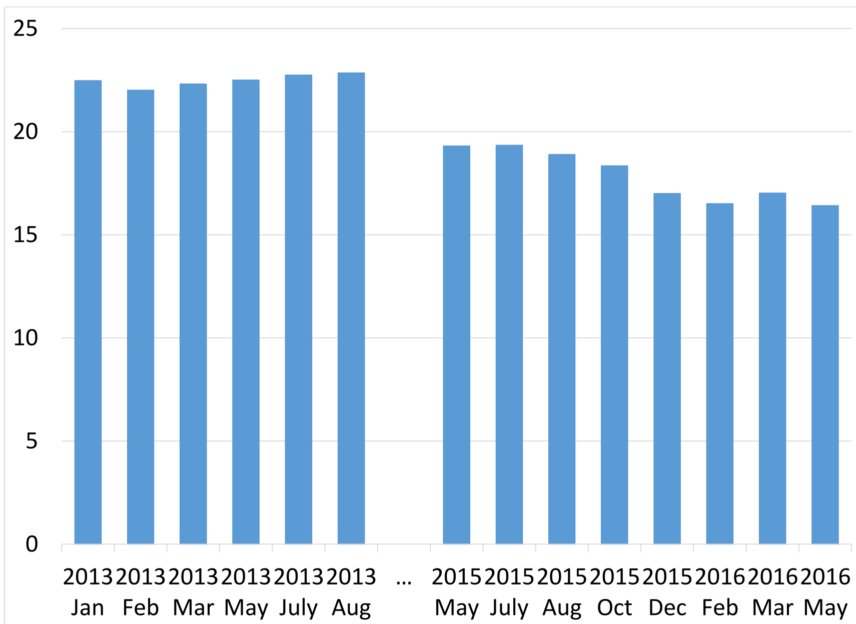

(c) Airport battery chargeable capacity in kWh

Figure 3.8: Airport battery degradation over time.

On the other hand, one fully charging/discharging cycle sample is extracted from each year to test sample efficiency. The data is listed in following TABLE 3.3. Here, SOC should start from very small value and rise to nearly 100%, then drop back to a similarly small number. The sample period in 2013 is detailed in Fig. 3.11. Fig. 3.8b represents the efficiencies computed from 4 samples in TABLE 3.3.

Both annual efficiency and sample efficiency (η) come from the ratio of discharged energy (E_d) to charged energy (E_c) for a time period $\mathcal{T}$. The equation is given at (3.1). E_c is corresponding to the sum of the negative battery output power, which is the charging power. Let us take the sample period in Fig. 3.11 for example. It is a round-trip because SOC started at 9.8% on May 7th and rise to 96% twice, ended at 9.8% again at May 14th. In η computation, $\sum_{\mathcal{T}} E_d$ is corresponding to integration of the part above zero, and $\sum_{\mathcal{T}} E_c$ is integration of the part below zero in battery power.

$$\eta = \frac{\sum_{\mathcal{T}} E_d}{-\sum_{\mathcal{T}} E_c} \tag{3.1}$$

Table 3.3: Airport battery round-trip samples

Year	Sample Period	SOC Range (%)	Efficiency
2013	May.7—May.14	9.8—96.0—9.8	83.81%
2014	Feb.15—Feb.28	15.9—99.3—14.8	88.13%
2015	Aug.1—Aug.8	1.5—99.4—1.5	75.99%
2016	Apr.17—Apr.22	1.4—99.3—1.6	76.34%

To check the battery chargeable capacity, all the fully charging processes are extracted from the 4-year database. The SOC criterion for selecting this sort of data is as close to 0—100% as possible. Data is presented in TABLE 3.4. Summing the power for each sample period we can carry out the charged energy in Fig. 3.8c. Notice that the rated battery capacity is 20 kWh. We can clearly see that it needed more than 22 kWh to achieve fully charged at the beginning. In 2016, 16 kWh was enough for it to get fully charged. Based on the three figures in Fig. 3.8, it is concluded that the degradation happened dramatically during 2014. The 4-year airport battery SOC data are plotted in Fig. 3.10. We notice that there was no fully charging/discharging operation for airport battery in 2014. From October 2014 to May 2015, the battery SOC was kept at low rate, 20% – 40%. That long-term low SOC status is harmful to battery health and eventually led to the dramatic degradation of the battery capacity.

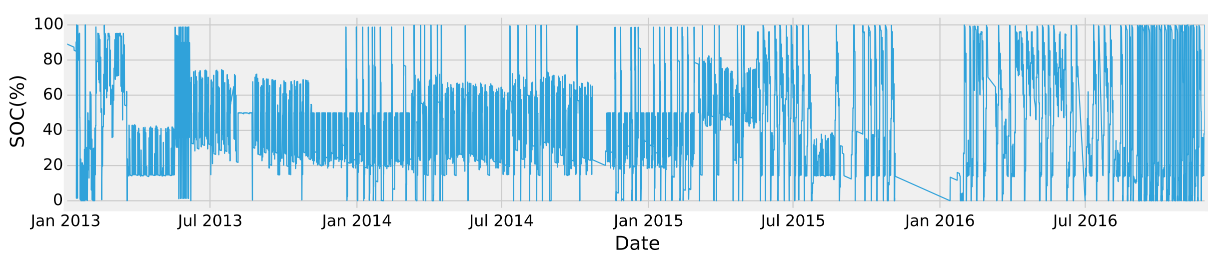

Figure 3.9: 2013-2016 Campus Battery SOC.

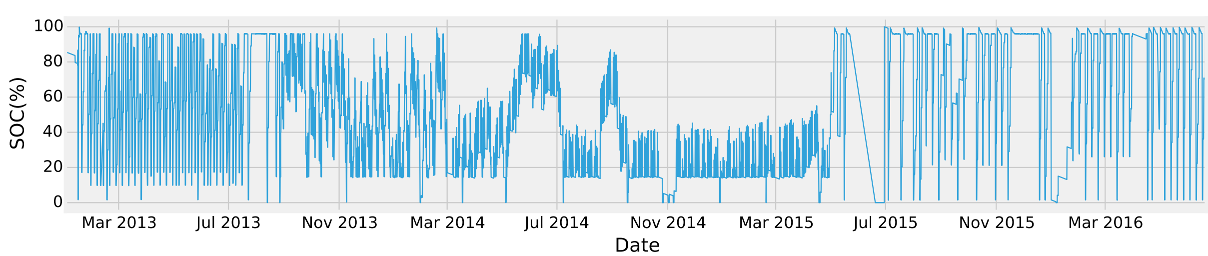

Figure 3.10: 2013-2016 Airport Battery SOC.

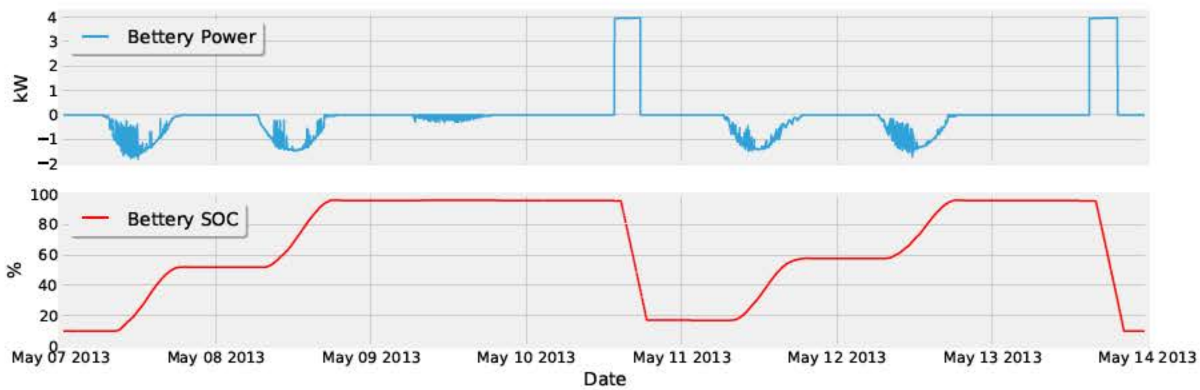

Figure 3.11: Airport battery sample period in 2013.

Table 3.4: Airport battery capacity of fully charged cases

Sample Period	SOC Range	Energy Charged(kWh)
2013-01-15 00:00—2013-01-15 23:59	1.7%-94.2%	22.47187025
2013-02-16 00:00—2013-02-18 13:00	2.0%-99.0%	22.01027732
2013-03-26 00:00—2013-03-28 23:59	1.8%-95.7%	22.30985377
2013-05-28 00:00—2013-05-30 23:59	1.6%-96.0%	22.49875008
2013-07-23 00:00—2013-07-26 12:00	1.5%-96.0%	22.743225
2013-08-13 00:00—2013-08-15 23:59	0.1%-96.0%	22.84445295
2015-05-16 00:00—2015-05-18 12:00	1.6%-99.4%	19.30745185
2015-07-04 00:00—2015-07-06 12:00	1.5%-99.3%	19.3391347
2015-08-08 00:00—2015-08-10 23:59	1.5%-99.2%	18.89023732
2015-10-10 00:00—2015-10-12 23:59	1.5%-99.4%	18.3444519
2015-12-19 00:00—2015-12-21 12:00	1.5%-99.4%	16.99893087
2016-02-08 00:00—2016-02-10 13:00	1.6%-99.2%	16.51102685
2016-03-14 00:00—2016-03-16 14:00	1.6%-99.2%	17.02032451
2016-05-27 00:00—2016-05-28 16:00	1.6%-99.4%	16.41198881

3.3 System Identification Analysis

Using the data collected, the USF SPS lab conducted research related to battery model identification. The research results have been posted in the Appendix.

Chapter 4

Course Work

A goal of SEEDS project is to integrate the research into teaching and student training. USF has developed a graduate level course "Energy Delivery Systems" to specifically address this goal. This course started in 2011. In Spring 2017, this course has become an official course EEL 4212 and registered in the Florida university course registry.

This course is offered every spring with enrollment of 30 $\sim$ 50 students. The course provides the students the fundamentals and analysis of the electric power delivery system to facilitate the integration of distributed energy resources, e.g. solar energy. This course covers renewable energy integration technology with a focus on power electronic converter control.

In this course, students will learn converter control for grid integration as well as simulation skills for demonstration. Below is a detailed list of learning outcomes.

1. Students will demonstrate the ability to conduct per unit conversion and power system circuit analysis to analyze power system operating conditions.

2. Students will be able to conduct analysis to design an energy delivery system for distributed energy resources using power electronic converters.

3. Student will demonstrate the knowledge of the fundamentals and operations of a microgrid through homework assignments, quiz and examination.

4. Students will demonstrate the knowledge of voltage sourced converters control design through course projects focused on simulation validation.

5. Students will be able to use power system simulation tools introduced in the class to conduct simulation validation.

The major topics include: (1) Fundamentals of electric distribution systems, (2) Power electronics systems for utility integration of the distributed energy resources, (3) Microgrid and its elements, (4) Voltage sourced converter (VSC) control and operation in a power delivery system, and (5) Operation and control of a Microgrid.

The SEEDS project is used as demos for students to understand a real-world PV and battery grid integration system. Not only students in the class have the opportunity to access the remote control panels of the two SEEDs site, but also the public has the chance to visit our lab and access the control panels and understand how grid integration works.

The following pi [illegible] PS lab to give in-class demo and tours to visitors.

Figure 4.1: Spring 2014 in-class demo.

Figure 4.2: Oct. 2016 international Roboticon event lab tour.

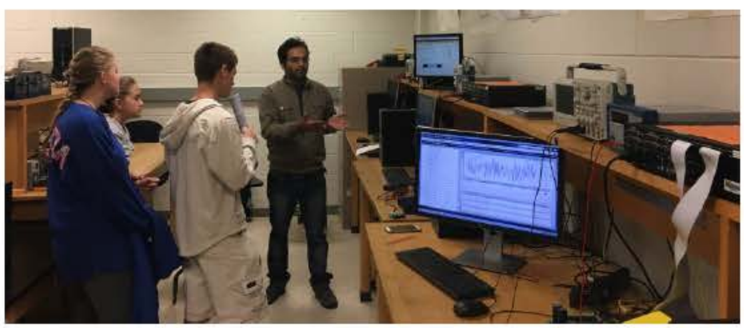

Figure 4.3: Feg. 2017 USF Engineering EXPO.

Appendix

System Identification

In recent years, batteries are used more and more. The target battery pack is located at St. Petersburg in Florida with the characteristics listed in TABLE 4.1. It serves as an energy storage device. It will be charged by Photovoltaic (PV) in the morning and discharged in the afternoon to mitigate electric power consuming. Fig. 4.4 shows the raw data obtained from meters, including measured terminal voltage (V_L), measured terminal current (I_L) and state-of-charge (SOC) in time-series. The time span is 22 days and sample time is 1 minute. The data extraction for analysis relies on data programming in Python.

Table 4.1: Battery Main Characteristics

Rated Capacity	20 kWh
Rated Power	5 kW
Cell Rated Capacity	400 Ah

This section has three objectives. The first one is to obtain SOC and open-circuit voltage (V_{OC}) relationship from voltage measurement and SOC data. The second one is to estimate SOC from current measurement. The third one is to estimate the equivalent circuit's RC parameters from measured current and SOC.

There are at least two major systematic methods for battery system estimation: Kalman filter based estimation and least-square estimation (LSE). For battery system identification, Kalman filter based estimation, including Extended Kalman filter (EKF) [1, 2], Unscented Kalman filter (UKF) [3, 4, 5], are widely used in state-of-charge (SOC) estimation and parameters identification. Kalman filter based method is a way to estimate the time-varying dynamic system with Gaussian noise. Kalman filter can be implemented online. On the other hand, LSE is chosen as a fast and efficient polynomial estimation method to identify battery system in [6, 7, 8]. By approximating derivatives by discrete data, discrete-time ARX models will be found. With an ARX model, A linear LSE problem can be formulated and the parameters of the ARX model can be carried out. In [9, 10], autoregressive exogenous (ARX) model are applied to generator system parameters identification. But there are very few papers to estimate battery systems parameters using ARX model.

The rest of the section is organized as follows. In subsection II, V_{OC} and SOC relationship will be obtained by using LSE non-linear regression. How to estimate SOC using current measurement and how to estimate the equivalent circuit's RC parameters are carried out using (ARX) model in subsection III and IV, respectively. In subection V, with the identified V_{OC} and SOC relationship,

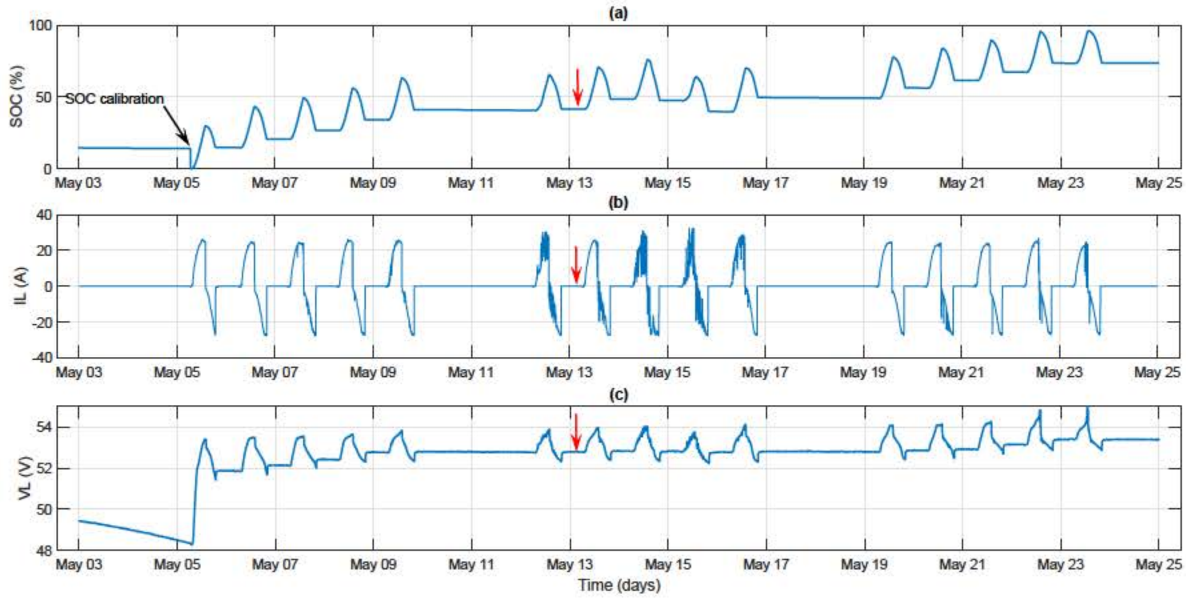

Figure 4.4: (a) State-of-charge (SOC). (b) Battery terminal current measurement. (c) Battery terminal voltage measurement.

RC parameters, we built a simulation model in MATLAB/Simpowersystems for validation. Finally, the conclusion is given in subection VI.

Estimation of open circuit voltage and SOC relationship

The relationship curve of open-circuit-voltage and SOC is usually used as a criterion to describe the battery health status. In [3, 8, 11, 12, 13], the experiment currents are constants to get V_{OC} under different SOC easily. However, the battery terminal current (I_L) and voltage (V_L) in our data vary with weather condition and power demand in real-time. The battery terminal voltage (V_L) only equals the open-circuit-voltage (V_{OC}) when no current flows and V_L is in steady state, as shown in Fig. 4.4 and pointed by the red arrows.

Normally, the open-circuit-voltage (V_{OC}) of a battery is greatly influenced by SOC, working temperature T and the number of cycles C, as shown in (4.1).

$$V_{OC} = f(SOC, \quad T, \quad C) \tag{4.1}$$

In our case, the V_{OC} and SOC is acquired at each early morning when the battery environment temperature varies little according to the history record. Also, considering 15 cycles in 22 days, the influence of cycle C can be neglected. Then (4.1) is simplified as (4.2). The triangle markers are used to represent the extracted 13 pairs of V_{OC} and SOC data in Fig. 4.5.

$$V_{OC} = f(SOC) \tag{4.2}$$

We can assume a target relationship function as a combination of exponential and polynomials. It is expressed in (4.3).

$$
\begin{aligned}
V_{OC} = & a \cdot e^{b \cdot SOC} + p_1 \cdot SOC^7 + p_2 \cdot SOC^6 + p_3 \cdot SOC^5 + \\
& p_4 \cdot SOC^4 + p_5 \cdot SOC^3 + p_6 \cdot SOC^2 + p_7 \cdot SOC + \\
& p_8
\end{aligned} \tag{4.3}
$$

We aim to find the coefficients: $a, b, p_1, ...p_8$ that can best fit the curve to the given data points. The objective function is

$$
\min_{a,b,p_1,\cdots,p_8} \sum_{i=1}^{n} (V_{OC}(a, b, p_1, \cdots, p_8) - V_{OCm})^2 \tag{4.4}
$$

where V_{OC} is the estimation from SOC, V_{OCm} is the voltage measurement.

By applying curve fitting toolbox in MATLAB, we get the coefficients of (4.3) and a single-variable function is used to represent the curve, as shown in (4.5).

$$
\begin{aligned}
V_{OC} = & - 4 \cdot e^{-0.3 \cdot SOC} + 9.431 \times 10^{-12} \cdot SOC^7 \\
& - 2.981 \times 10^{-9} \cdot SOC^6 + 3.541 \times 10^{-7} \cdot SOC^5 \\
& - 1.899 \times 10^{-5} \cdot SOC^4 + 3.965 \times 10^{-4} \cdot SOC^3 \\
& + 9.775 \times 10^{-4} \cdot SOC^2 - 0.08582 \cdot SOC + 52.32
\end{aligned} \tag{4.5}
$$

This function is plotted in Fig. 4.5 and it is shown that the curve fits the data points very well.

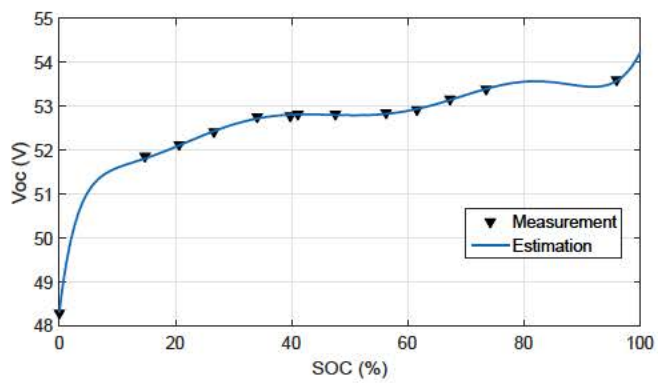

Figure 4.5: SOC vs. V_{OC} measured and estimation curve.

SOC estimation

In this Section, the general discrete-time ARX model structure will be first explained. SOC estimation and current measurement (I_L) relationship will be converted to discrete time based on Coulomb counting method. With applying ARX model to derivatives, the I_L to SOC transfer function will be carried out by LSE.

ARX model structure

A general polynomial ARX model structure can be expressed as equation (4.6):

$$A(z)y(k) = B(z)u(k - n_k) + e(k) \tag{4.6}$$

where

- $u(k)$ is the system inputs.
- $y(k)$ is the system outputs.
- n_k is the system delay.
- $e(k)$ is the White-noise system disturbance.
- $A(z)$ and $B(z)$ are polynomial with k_a and k_b orders respect to the backward shift operator z^{-1} and defined by the following equations:

$$A(z) = 1 + a_1 z^{-1} + \cdots + a_{k_a} z^{-k_a} \tag{4.7}$$
$$B(z) = b_0 + b_1 z^{-1} + \cdots + b_{k_b-1} z^{-(k_b-1)} \tag{4.8}$$

Fig. 4.6 depicts the signal flow of an ARX model. Given time series no-delay ($n_k = 0$) measurements of the input and output, say from k step to N step, an overestimated problem can be formulated as (4.9) based on (4.6):

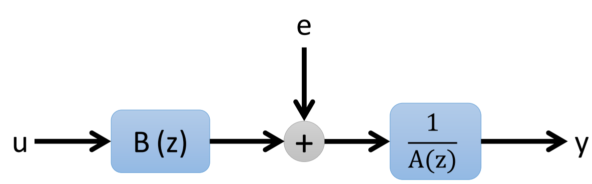

Figure 4.6: ARX model signal flowchart.

$$\begin{bmatrix} y(k) \\ y(k+1) \\ \dots \\ y(N) \end{bmatrix} = \begin{bmatrix} y(k-1) & y(k-2) & \dots & y(k-k_a) & u(k) & u(k-1) & \dots & u(k-(k_b-1)) \\ y(k-2) & y(k-3) & \dots & y(k-k_a-1) & u(k-1) & u(k-2) & \dots & u(k-k_b) \\ \vdots & \vdots & \ddots & \vdots & \vdots & \vdots & \ddots & \vdots \\ y(N-1) & y(N-2) & \dots & y(N-k_a) & u(N) & u(N-1) & \dots & u(N-(k_b-1)) \end{bmatrix} \begin{bmatrix} -a_1 \\ \vdots \\ -a_{ka} \\ b_0 \\ b_1 \\ \vdots \\ b_{k_b-1} \end{bmatrix} + e(k) \tag{4.9}$$

ARX model-based SOC estimation

Theoretically, state of charge is a relative quantity that describes the ratio of the remaining capacity to the nominal capacity of a battery. The Coulomb counting is a method developed from this concept, which estimates SOC by an measurement of total current accumulation. It can be given by:

$$SOC = SOC_0 + \frac{\int \eta I_L dt}{C_N} \tag{4.10}$$

where SOC_0 is the initial value of the SOC, η is the Coulombic efficiency, and C_N is the nominal capacity.

In our case, the battery had been fully discharged and experienced a long time of self-discharge to calibrate the initial value of SOC. Shown from Fig. (4.8), I_L kept zero while V_L kept decreasing before May 5th attribute to the effect of battery self-discharge. The SOC_0 was calibrated to zero on May 5th as shown in Fig. (4.8) (a) and pointed by the black arrow.

Convert (4.10) to discrete-time as:

$$SOC(k) = SOC(k-1) + \frac{\eta \Delta t}{C_N} I_L(k-1) \tag{4.11}$$

Assume $\frac{\eta \Delta t}{C_N}$ as a constant number b_1. From (4.11), the transfer function can be expressed by:

$$\frac{y}{u} = \frac{b_1 z^{-1}}{1 - z^{-1}} \tag{4.12}$$

Applying this to discrete-time ARX model, we can get the transfer function with order of [1 1 1]. This yields to

$$A(z)SOC(k) = B(z)I_L(k) + e(k) \tag{4.13}$$

where

$$A(z) = 1 - z^{-1}$$
$$B(z) = 0.004615z^{-1}$$

With above discrete ARX transfer function, SOC estimation can be expressed as:

$$SOC(k) = SOC(k-1) + 7.69 \times 10^{-5} \Delta t \cdot I_L(k-1) + e(k) \tag{4.14}$$

where

$$SOC(0) = 0$$
$$\Delta t = 60 seconds$$

Given I_L as input, we can compare ARX model based SOC simulation output with SOC raw data in Fig. 4.7. The Simulated ARX model output fits raw data very well with 98.59% fitting degree and 0.06522 mean-square error(MSE).

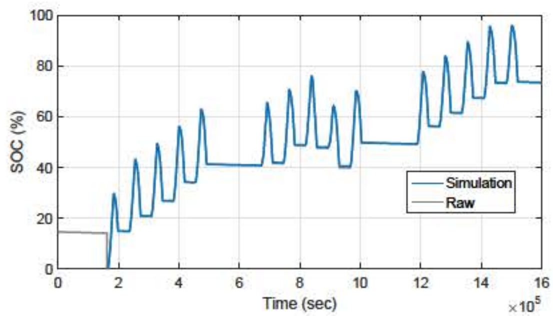

Figure 4.7: Comparison of SOC ARX model simulation output and SOC raw data.

Equivalent circuit parameters identification

In this section, the battery equivalent circuit is first proposed. The Dynamic equations of two RC branches are converted to discrete-time in z domain. Finally, estimation of ARX Model coefficients are carried out and RC parameters recovery is conducted with physical meaning.

Equivalent circuit modeling

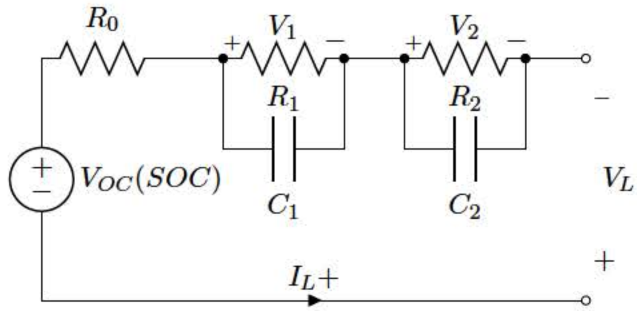

Figure 4.8: Schematic of the battery equivalent circuit.

Among battery equivalent circuits, the Thevenin-based model is widely used in [3, 8, 11, 14, 15, 16, 12, 17] since it can not only bridge SOC to open-circuit voltage, but also simulate the transient response of load changing. It consists of two parts. One part is open-circuit voltage(V_{OC}), which in function of state-of-charge (SOC) as shown in Eq. (4.5). V_{OC} is presented by a voltage-controlled voltage source in Fig. 4.8. Another part is the RC network, including one ohmic resistance R_0 and two paralleled RC branches (R_1, C_1 and R_2, C_2), are responsible for short-time and long-time constants of the step response. The proposed equivalent model is a trade off between accuracy and complexity.

Discretization of dynamic equations

As assumed in Fig. 4.8, I_L is the terminal current with a positive value in charge process and negative value in discharge process. Two RC parallel branches in proposed model can be expressed as following differential equations:

$$C_1\frac{dV_1(t)}{dt} = \frac{-V_1(t)}{R_1} + I_L \tag{4.15}$$

$$C_2\frac{dV_2(t)}{dt} = \frac{-V_2(t)}{R_2} + I_L \tag{4.16}$$

Rewrite (4.15) and (4.16) as:

$$\dot{V_1} = \frac{-1}{R_1C_1}V_1 + \frac{1}{C_1}I_L \tag{4.17}$$

$$\dot{V_2} = \frac{-1}{R_2C_2}V_2 + \frac{1}{C_2}I_L \tag{4.18}$$

The state space model is:

$$\begin{bmatrix}\dot{V_1}\\ \dot{V_2}\end{bmatrix} = \underbrace{\begin{bmatrix}\frac{-1}{R_1C_1} & 0\\ 0 & \frac{-1}{R_2C_2}\end{bmatrix}}_{\text{A}} \times \begin{bmatrix}V_1\\ V_2\end{bmatrix} + \underbrace{\begin{bmatrix}\frac{1}{C_1}\\ \frac{1}{C_2}\end{bmatrix}}_{\text{B}} \times I_L \tag{4.19}$$

$$V_L - V_{OC} = \underbrace{\begin{bmatrix}1 & 1\end{bmatrix}}_{\text{C}} \times \begin{bmatrix}V_1\\ V_2\end{bmatrix} + \underbrace{R_0}_{\text{D}} \times I_L \tag{4.20}$$

From (4.19) and (4.20) we have the expression as:

$$\dot{x} = Ax + Bu \tag{4.21}$$

$$y = Cx + Du \tag{4.22}$$

where $x = \begin{bmatrix}V_1\\ V_2\end{bmatrix}$, $u = I_L$ is the input, and $y = V_L - V_{OC}$ is the output. We can get the V_{OC} from (4.5). A discrete-time form of (4.21) is arranged as (4.23), where k = 1,2,3 . . .

$$x(k+1) = x(k) + (Ax(k) + Bu(k)) \cdot h \tag{4.23}$$

where h is time interval. Substitute x(k+1) by $z \cdot x(k)$:

$$z \cdot x(k) = x(k) + (AH + I) \cdot x(k) + Bh \cdot u(k) \tag{4.24}$$

$$x(k) = [zI - (Ah + I)]^{-1}Bh \cdot u(k) \tag{4.25}$$

For the output, substitute (4.25) into (4.22):

$$y(k) = C \cdot [zI - (Ah + I)]^{-1}Bh \cdot u(k) + D \cdot u(k) \tag{4.26}$$

$$y(k) = (C \cdot [zI - (Ah + I)]^{-1}Bh + D) \cdot u(k) \tag{4.27}$$

$$\frac{y(k)}{u(k)} = C \cdot [zI - (Ah + I)]^{-1} Bh + D \tag{4.28}$$

The corresponding transfer function $G(z)$ of (4.28) is:

$$G(Z^{-1}) = \frac{b_0 + b_1 z^{-1} + b_2 z^{-2}}{1 + a_1 z^{-1} + a_2 z^{-2}} \tag{4.29}$$

where a_1, a_2, b_0, b_1 and b_2 are the coefficients relate to RC parameters (4.30)~(4.34). In our measurement data, time interval h is 60 seconds.

$$a_1 = \frac{h}{R_1C_1} + \frac{h}{R_2C_2} - 2 \tag{4.30}$$

$$a_2 = -\frac{h}{R_1C_1} - \frac{h}{R_2C_2} + \frac{h^2}{R_1R_2C_1C_2} + 1 \tag{4.31}$$

$$b_0 = R_0 \tag{4.32}$$

$$b_1 = \frac{h}{C_1} + \frac{h}{C_2} + \frac{hR_0}{R_1C_1} + \frac{hR_0}{R_2C_2} - 2R_0 \tag{4.33}$$

$$\begin{aligned} b_2 = R_0 &+ \frac{h^2}{R_1C_1C_2} + \frac{h^2}{R_2C_1C_2} + \frac{h^2R_0}{R_1R_2C_1C_2} \\ &- \frac{h}{C_1} - \frac{h}{C_2} - \frac{hR_0}{R_1C_1} - \frac{hR_0}{R_2C_2} \end{aligned} \tag{4.34}$$

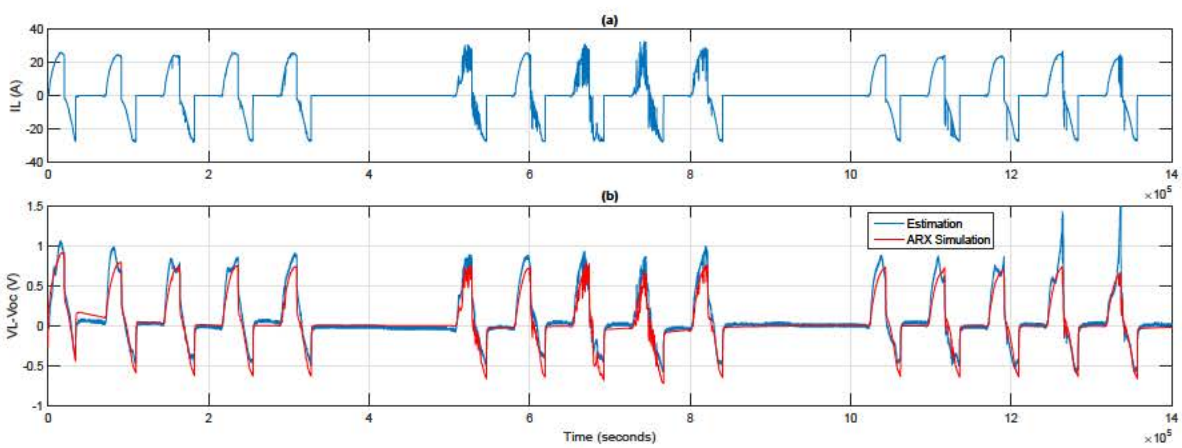

Figure 4.9: (a) ARX model input I_L. (b) Comparison of $V_L - V_{OC}$ estimation and ARX model simulation

ARX model-based RC estimation

In this case, the setting of ARX model is assumed as following:

$$A(z)y(k) = B(z)u(k) + e(k) \tag{4.35}$$

where

$$A(z) = 1 + a_1 z^{-1} + a_2 z^{-2}$$
$$B(z) = b_0 + b_1 z^{-1} + b_2 z^{-2}$$

- Inputs: $u(k) = I_L$
- Outputs: $y(k) = V_L - V_{oc}$
- Sample time: $T_s = 60$ seconds
- Total time: $S = 19$ days
- Order of the polynomial $A(z)$: $k_a = 2$
- Order of the polynomial $B(z) + 1$: $k_b = 3$
- Input-output delay: $n_k = 0$

Using Matlab identification toolbox we can solve ARX Model with 68.82% simulation focus and 0.0099 mean-square-error (MSE). The ARX model simulated output and $V_L - V_{OC}$ evaluated output are compared and shown in Fig. 4.9. And the transfer function we can get is:

$$G(Z^{-1}) = \frac{0.009229 - 0.01419z^{-1}0.004967z^{-2}}{1 - 1.817z^{-1} + 0.8168z^{-2}} \tag{4.36}$$

Applying the 3th, 10th and 16th days data, into $(V_L - V_{oc})$ ARX model to validate the reliability of coefficients we got in (4.36). All these three groups coefficients are compared and listed in TABLE 4.2, shown that the variation of coefficients is acceptable so (4.36) is reliable to identify equivalent circuit parameters.

Table 4.2: ARX Model Coefficients from Different Time Periods

a, b	19 days	3th day	10th day	16th day	Max Error
a_1	-1.817	-1.879	-1.876	-1.887	3.8%
a_2	0.8186	0.8789	0.8759	0.8872	8.3%
b_0	0.009229	0.009308	0.008698	0.00833	9.7%
b_1	-0.01419	-0.01584	-0.01464	-0.01401	11.6%
b_2	0.0049676	0.006543	0.005945	0.005675	31.7%

Substitute the coefficients in (4.36) into the system of equations (4.30)-(4.34). We can get the solution of circuit RC parameters are $R_0 = 0.009188\Omega$, $R_1 = 0.0068\Omega$, $R_2 = 0.0140\Omega$, $C_1 = 7.926 \times 10^6 F$, $C_2 = 2.38 \times 10^4 F$. In TABLE 4.3, the RC parameters which estimated from different periods are listed. Theoretically, the RC parameters are multi-variable functions of current, SOC, temperature and cycle number. It will lead the RC parameters variation without considering above all factors.

Table 4.3: RC Parameters Estimated from Different Time Periods

R, C	19 days	3th day	10th day	16th day
$R_1(\Omega)$	0.0529	0.1320	0.0518	0.0495
$R_2(\Omega)$	0.0137	0.0127	0.0131	0.0162
$R_0(\Omega)$	0.009229	0.009308	0.008698	0.00833
$C_1(F)$	1.04×10^6	5.54×10^5	1.4454×10^6	6.74×10^5
$C_2(F)$	2.38×10^4	3.89×10^4	3.67×10^4	3.33×10^4

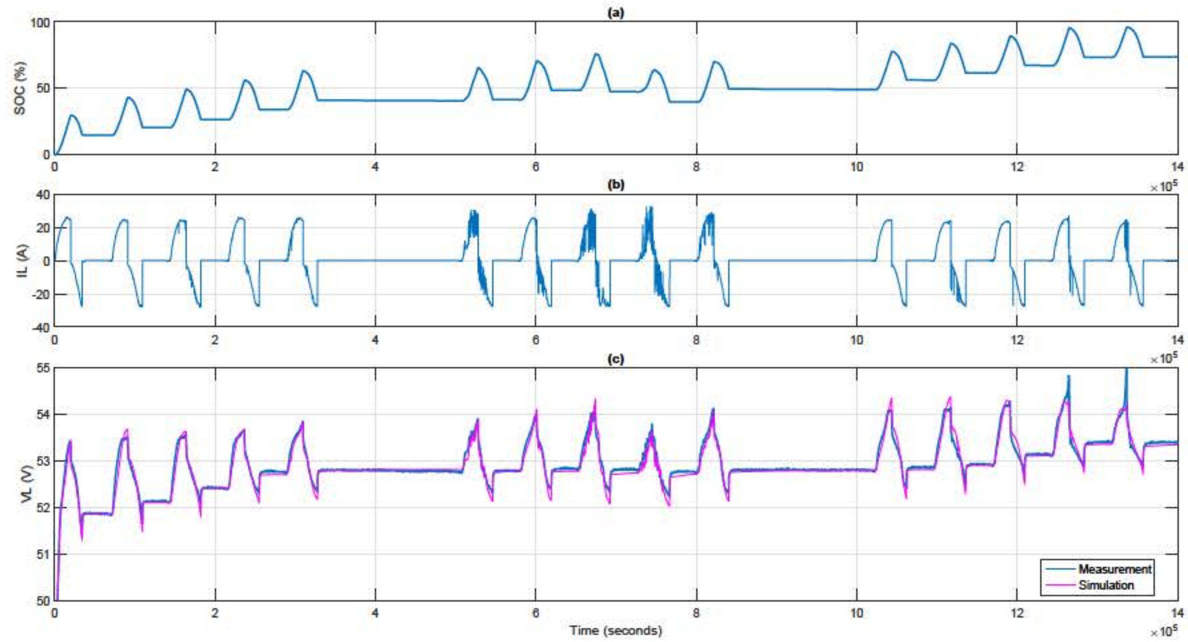

Figure 4.10: (a) State-of-charge (SOC). (b) I_L input for current source. (c) Comparison of voltage measurement data and voltage simulation.

Validation testbed

A simulation model, which shown as Fig.(4.11), was built to to validate the proposed battery model performance. In this model, we set SOC and current (I_L) as two inputs. V_{OC} is in function of SOC in (4.5) as a voltage-controlled voltage source. I_L is the original measurement current acting as current source on terminal side. Then measure the simulation model terminal voltage (V_L) and compare it with the original battery measured voltage. All the inputs and outputs are presented in Fig.(4.10). By comparing the results, the mean squared error (MSE) is $0.01V$. The simulation measured DC voltage fit to raw measured DC voltage very well.

Conclusion

In this brief, system identification progress has been carried out for a 20 kW.h battery pack using real-world measurement data. State-of-charge (SOC) and open-circuit voltage (V_{OC}) relationship

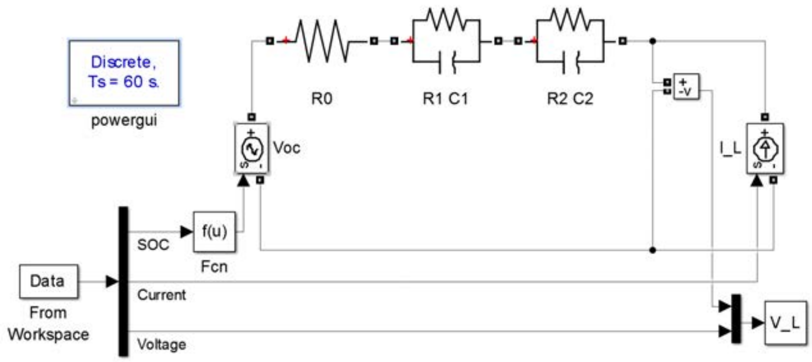

Figure 4.11: Simulation testbed for validation.

has been obtained by using least square estimation (LSE) non-linear regression. In addition, how to estimate SOC using current measurement and how to estimate the equivalent circuit's RC parameters were carried out using ARX model. Finally, with the identified V_{OC} to SOC relationship and RC parameters, we built a simulation model in MATLAB/Simpowersystems. With the measured current data from the real-world as the input, the simulation model gives the terminal DC voltage as the output. This output is compared with the real-world DC voltage measurement data and the matching degree is satisfactory.

The deviation in the simulation is attribute to two main reasons. One is SOC estimation by Coulomb counting has flaws of accumulation of measurement errors due to uncertain disturbances and difficulty determine the initial value of SOC accurately. SOC needs to be calibrated periodically just like the beginning of raw data. Uncertain SOC has a significant effect on battery system identification. Another reason is without considering the temperature influence on battery internal electrochemical characteristics, which leading deviation of RC parameters in different sample periods.

Python code

Table 1.1

Table 1.1 was generated using the following Python code running in Python Notebook (Fig. 4.12).

PV Power Histogram

The following Python code aims to open the database, make queries, fetch data and make plots. The codes are as follows.

```
import sqlite3
import time
import datetime
import random

import pylab
import matplotlib.pyplot as plt
```

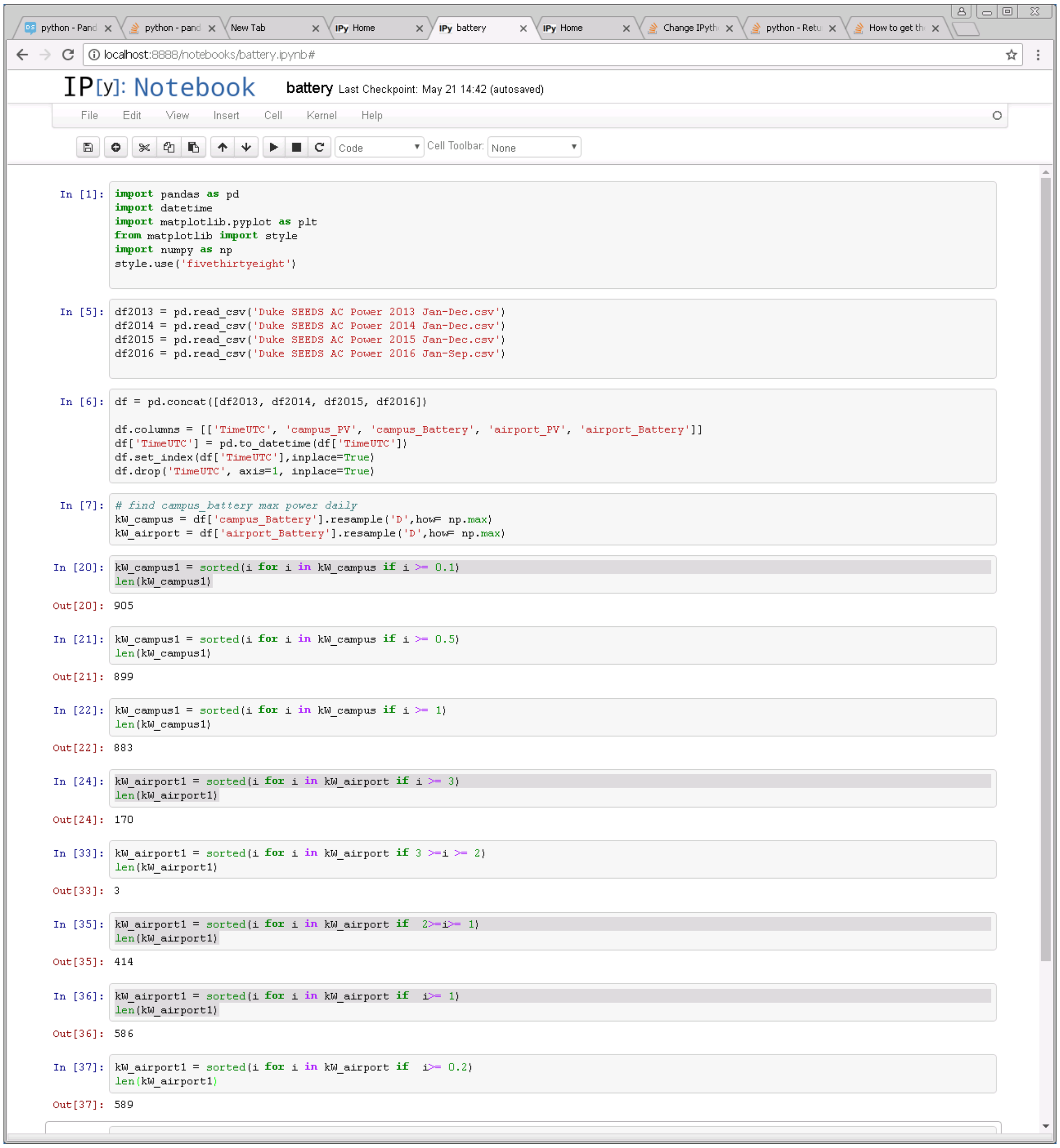

Figure 4.12: Table 1.1.

```
import matplotlib.dates as mdates
from dateutil import parser
from matplotlib import style
style.use('fivethirtyeight')

conn = sqlite3.connect('Duke SEEDSv1.db')
c = conn.cursor()

def graph_data():
    c.execute('SELECT strftime("%Y-%m-%d", TimeUTC), sum(ch01635_Avg_kW)/60, sum(ch01648_Avg_kW)/60\
               FROM "Duke SEEDS AC Power 2016 Jan-Sep"\
               WHERE date(TimeUTC)<("2016-06-15")\
```

```
                GROUP BY strftime("%Y-%m-%d", TimeUTC)')
    data = c.fetchall()

    dates = []
    values1 = []
    values2 = []

    for row in data:
        dates.append(parser.parse(row[0]))
        values1.append(row[1])
        values2.append(row[2])

    #plt.plot_date(dates,values1,'-')
    #plt.title('ch01648_Avg_Power')
    #plt.xlabel('Date');
    #plt.ylabel('Daily accumulated energy');
    #plt.show()
    bins = range(13);
    plt.figure()
    plt.hist(values1, bins, normed=1, histtype='bar', rwidth=0.8);
    plt.xlabel('kWh');
    plt.ylabel('Probability');

    plt.title('2016 Campus PV');#plt.show();
    plt.savefig('figure_pv1.eps')
    plt.show()
    plt.figure()
    plt.hist(values2, bins, normed=1, histtype='bar', rwidth=0.8);
    plt.xlabel('kWh');
    plt.ylabel('Probability');
    plt.title('2016 Airport PV');
    plt.show()
    plt.savefig('figure_pv2.eps')

def read_from_db():
    c.execute('SELECT strftime("%Y-%m-%d", TimeUTC), sum(ch01648_Avg_kW)/60\
                FROM "Duke SEEDS AC Power 2013 Jan-Dec"\
                WHERE date(TimeUTC)<("2013-02-01")\
                GROUP BY strftime("%Y-%m-%d", TimeUTC)')
    data = c.fetchall()
    print(data)
    for row in data:
        print(row)


#create_table()
#data_entry()
#dynamic_data_entry()

read_from_db()
graph_data()
c.close
conn.close()
```

PV, Battery and Total Power Plots

The following Python codes are for PV, battery and total power plotting.

```
import sqlite3
import time
import datetime
import random


import matplotlib.pyplot as plt
import matplotlib.dates as mdates
from dateutil import parser
from matplotlib import style
style.use('fivethirtyeight')

conn = sqlite3.connect('Duke SEEDSv1.db')
c = conn.cursor()

def graph_data():
    c.execute('SELECT TimeUTC, ch01635_Avg_kW, ch06401_Avg_kW, ch01648_Avg_kW, ch06414_Avg_kW\
                FROM "Duke SEEDS AC Power 2013 Jan-Dec"\
                WHERE date(TimeUTC)<("2013-07-24") AND date(TimeUTC)>("2013-07-21")')
    data = c.fetchall()

    dates = []
    PV1_power = [];
    PV2_power =[];
    B1_power =[]
    B2_power =[];
    total1_power =[]
    total2_power =[]
    print(data[0]);
    for row in data:
        dates.append(parser.parse(row[0]))
        PV1_power.append(row[1])
        B1_power.append(row[2])
        PV2_power.append(row[3])
        B2_power.append(row[4])
        total1_power.append(row[1]+row[2]);
        total2_power.append(row[3]+row[4]);

    print("done");
    plt.figure(figsize=(20,8))
    plt.plot_date(dates,PV1_power,'b-')
    plt.plot_date(dates,B1_power,'r-')
    plt.plot_date(dates,total1_power, 'g-')
    plt.xlabel('Time');
    plt.ylabel('kW');
    plt.title('Campus site')
    plt.savefig('fig1.png')
    plt.show()

    plt.figure(figsize=(20,8))
    plt.plot_date(dates,PV2_power,'b-')
    plt.plot_date(dates,B2_power,'r-')
```

```
    plt.plot_date(dates,total2_power, 'g-')
    plt.xlabel('Time');
    plt.ylabel('kW');
    plt.title('Airport site')
    plt.savefig('fig2.png')
    plt.show()
def read_from_db():
    c.execute('SELECT TimeUTC, ch06401_Avg_kW\
                FROM "Duke SEEDS AC Power 2013 Jan-Dec"\
                WHERE date(TimeUTC)<("2013-02-01") AND date(TimeUTC)>("2013-01-21")')
    data = c.fetchall()
    #print(data)
    #for row in data:
    #    print(row)


#create_table()
#data_entry()
#dynamic_data_entry()

#read_from_db()
graph_data()
c.close
conn.close()
```

Battery Energy Plots

The following codes cll Python pandas and directly call four csv files that store EPRI data. This particular code gives the plot of the airport battery data. Change the channel name to be "ch06401_Avg_kW", then we can obtain the campus batter's plot.

```
import pandas as pd
import datetime
import matplotlib.pyplot as plt
from matplotlib import style

style.use('fivethirtyeight')

fig = plt.figure()
ax1 = plt.subplot2grid((1,1), (0,0))

df2013 = pd.read_csv('Duke SEEDS AC Power 2013 Jan-Dec.csv', usecols=[0, 4])
df2014 = pd.read_csv('Duke SEEDS AC Power 2014 Jan-Dec.csv', usecols=[0, 4])
df2015 = pd.read_csv('Duke SEEDS AC Power 2015 Jan-Dec.csv', usecols=[0, 4])
df2016 = pd.read_csv('Duke SEEDS AC Power 2016 Jan-Sep.csv', usecols=[0, 4])

df = pd.concat([df2013, df2014, df2015, df2016])
#df = df2013;
df['TimeUTC'] = pd.to_datetime(df['TimeUTC'])
df.set_index(df['TimeUTC'],inplace=True)
df = df.drop('TimeUTC', axis=1)

df['ch06414_Charge_kWh'] = df.ch06414_Avg_kW[df['ch06414_Avg_kW'] > 0]/60
df['ch06414_Discharge_kWh'] = df.ch06414_Avg_kW[df['ch06414_Avg_kW'] < 0]/60
```

```
df['Daily_Charge_kWh'] = df.ch06414_Charge_kWh.resample('D').sum()
df['Daily_Discharge_kWh'] = df.ch06414_Discharge_kWh.resample('D').sum()

df = df[['Daily_Charge_kWh', 'Daily_Discharge_kWh']]
df.dropna(inplace=True)
df['Diff'] = df['Daily_Charge_kWh'] + df['Daily_Discharge_kWh']
print (df)

#df['Diff'].plot(ax=ax1)
df['Daily_Charge_kWh'].plot(ax=ax1,kind='line')
df['Daily_Discharge_kWh'].plot(color='g',ax=ax1,kind='line')
plt.legend()
plt.title('Albert Whitted Park / Greensmith Energy Storage(kWh)')
plt.show()
```

Bibliography

[1] J. Lee, O. Nam, and B. Cho, "Li-ion battery soc estimation method based on the reduced order extended kalman filtering," *Journal of Power Sources*, vol. 174, no. 1, pp. 9–15, 2007.

[2] G. L. Plett, "Extended kalman filtering for battery management systems of lipb-based hev battery packs: Part 3. state and parameter estimation," *Journal of Power sources*, vol. 134, no. 2, pp. 277–292, 2004.

[3] H. He, R. Xiong, X. Zhang, F. Sun, and J. Fan, "State-of-charge estimation of the lithium-ion battery using an adaptive extended kalman filter based on an improved thevenin model," *IEEE Transactions on Vehicular Technology*, vol. 60, no. 4, pp. 1461–1469, 2011.

[4] J. Han, D. Kim, and M. Sunwoo, "State-of-charge estimation of lead-acid batteries using an adaptive extended kalman filter," *Journal of Power Sources*, vol. 188, no. 2, pp. 606–612, 2009.

[5] F. Sun, X. Hu, Y. Zou, and S. Li, "Adaptive unscented kalman filtering for state of charge estimation of a lithium-ion battery for electric vehicles," *Energy*, vol. 36, no. 5, pp. 3531–3540, 2011.

[6] G. L. Plett, "Recursive approximate weighted total least squares estimation of battery cell total capacity," *Journal of Power Sources*, vol. 196, no. 4, pp. 2319–2331, 2011.

[7] X. Hu, F. Sun, Y. Zou, and H. Peng, "Online estimation of an electric vehicle lithium-ion battery using recursive least squares with forgetting," in *American Control Conference (ACC), 2011*. IEEE, 2011, pp. 935–940.

[8] H. He, X. Zhang, R. Xiong, Y. Xu, and H. Guo, "Online model-based estimation of state-of-charge and open-circuit voltage of lithium-ion batteries in electric vehicles," *Energy*, vol. 39, no. 1, pp. 310–318, 2012.

[9] B. Mogharbel, L. Fan, and Z. Miao, "Least squares estimation-based synchronous generator parameter estimation using pmu data," in *Power & Energy Society General Meeting, 2015 IEEE*. IEEE, 2015, pp. 1–5.

[10] Y. Xu, Z. Miao, and L. Fan, "Deriving arx models for synchronous generators," in *North American Power Symposium (NAPS), 2016*. IEEE, 2016, pp. 1–6.

[11] M. Chen and G. A. Rincon-Mora, "Accurate electrical battery model capable of predicting runtime and iv performance," *IEEE transactions on energy conversion*, vol. 21, no. 2, pp. 504–511, 2006.

[12] B. Schweighofer, K. M. Raab, and G. Brasseur, “Modeling of high power automotive batteries by the use of an automated test system,” *IEEE Transactions on Instrumentation and Measurement*, vol. 52, no. 4, pp. 1087–1091, 2003.

[13] A. Szumanowski and Y. Chang, “Battery management system based on battery nonlinear dynamics modeling,” *IEEE transactions on vehicular technology*, vol. 57, no. 3, pp. 1425–1432, 2008.

[14] L. Xu, Z. Miao, and L. Fan, “Control of a battery system to improve operation of a microgrid,” in *Power and Energy Society General Meeting, 2012 IEEE*. IEEE, 2012, pp. 1–8.

[15] V. Johnson, “Battery performance models in advisor,” *Journal of power sources*, vol. 110, no. 2, pp. 321–329, 2002.

[16] C. Zhang, J. Liu, S. Sharkh, and C. Zhang, “Identification of dynamic model parameters for lithium-ion batteries used in hybrid electric vehicles,” 2010.

[17] L. Gao, S. Liu, and R. A. Dougal, “Dynamic lithium-ion battery model for system simulation,” *IEEE transactions on components and packaging technologies*, vol. 25, no. 3, pp. 495–505, 2002.

ATTACHMENT D

Measures	Project Costs	Cost-effectiveness Test Results	Incentive Amount
Lighting, HVAC	$7,576.00	1.01	$2,200.00
Lighting, HVAC	$419,000.00	1.06	$19,673.00
Lighting, HVAC, Windows	$111,566.00	1.10	$27,622.00
Lighting, HVAC, Windows	$114,630.42	1.09	$23,576.00
Lighting, HVAC, Windows	$114,630.42	1.08	$24,001.00
Lighting and Chilled Beam	$1,356,996.00	1.04	$8,972.90
Lighting and DCV	$203,385.00	1.04	$10,705.09
Lighting, HVAC	$47,033.00	1.07	$2,074.72
Lighting, HVAC	$38,764.00	1.05	$3,282.24
Lighting, HVAC	$84,246.00	1.01	$19,100.00
Lighting, HVAC	$12,737.00	1.01	$568.43
Lighting, HVAC	$9,075.00	1.02	$354.00
Lighting, HVAC	$11,287.00	1.03	$484.00
Lighting, HVAC	$14,270.00	1.01	$1,057.81
Lighting, HVAC, Cool Roof	$14,270.00	1.01	$1,057.81
Lighting, HVAC, Cool Roof	$14,270.00	1.01	$1,057.81
Lighting, HVAC	$168,513.00	1.04	$12,500.00
Lighting, HVAC	$224,867.00	1.04	$9,183.35
Lighting, HVAC	$209,372.00	1.04	$10,479.00
Lighting, HVAC	$225,266.00	1.05	$4,953.96
Lighting, HVAC	$163,488.00	1.05	$10,697.33
Lighting, HVAC	$167,977.00	1.05	$10,615.73
Lighting, HVAC	$214,999.00	1.05	$11,019.82
Lighting, HVAC	$188,421.00	1.04	$11,801.99
Lighting, HVAC	$159,076.00	1.05	$11,419.98
Lighting, HVAC	$204,331.00	1.04	$12,840.33

Lighting, HVAC	$174,616.00	1.05	$10,775.59
Lighting, HVAC	$213,248.00	1.05	$8,542.97
Lighting, HVAC	$70,359.00	1.03	$1,616.00